Accepted Manuscript

Title: Piezoelectric materials for catalytic/photocatalytic removal of pollutants: recent advances and outlook

Authors: Zhang Liang, Chang-Feng Yan, Sami Rtimi, Jayasundera Bandara

Please cite this article as: Liang Z, Yan C-Feng, Rtimi S, Bandara J, Piezoelectric materials for catalytic/photocatalytic removal of pollutants: recent advances and outlook, *Applied Catalysis B: Environmental* (2018), https://doi.org/10.1016/j.apcatb.2018.09.028

Piezoelectric materials for catalytic/photocatalytic removal of pollutants: recent advances and outlook

Zhang Liang[1], Chang-Feng Yan[1]*, Sami Rtimi[2], Jayasundera Bandara[3]*

[1] Hydrogen Production and Utilization Laboratory, Key Laboratory of Renewable Energy, Guangzhou Institute of Energy Conversion, Chinese Academy of Sciences, Guangzhou, 510640, China
[2] Swiss Federal Institute of Technology, Advanced Oxidation Processes Group (GPAO), EPFL-SB-ISIC-GPAO, 1015 Lausanne, Switzerland
[3] National Institute of Fundamental Studies, Hantana Road, CP 20000, Kandy, Sri Lanka

*Correspondence to: Jayasundera Bandara: bandaraj@ifs.ac.lk ; jayasundera@yahoo.com

Chang-Feng Yan: yancf@ms.giec.ac.cn

Graphical abstract:

Piezo-catalysis   Piezoelectric   Piezo-photocatalysis
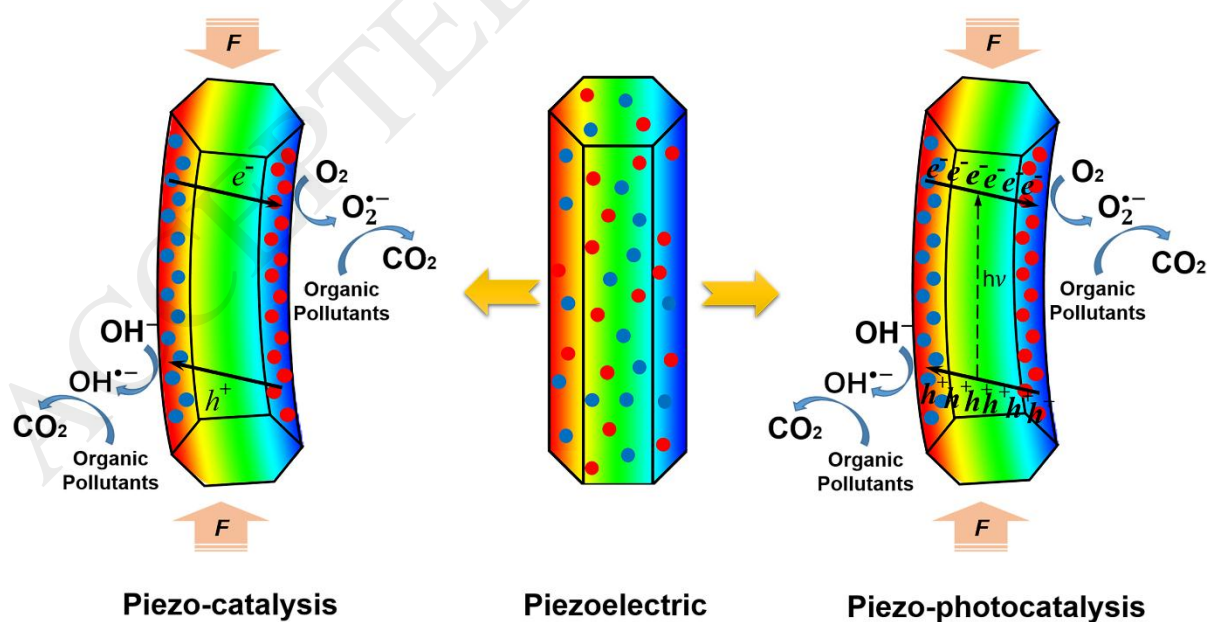
Highlights :

- photocatalytic oxidation of organic contaminants is reviewed in the present study

- Ferroelectric, pyroelectric and piezoelectric effects of photocatalytic materials was exploited

- Due to non-centrosymmetric nature, the piezoelectric materials showed catalytic properties.

- Applications of piezoelectric materials in environmental remediation are reviewed.

Abstract

The accumulation of various contaminants in air, soil and water is threatening the natural environment. The remediation of the environmental contaminations is today an urge. Among the remediation methods employed, advanced oxidation processes (AOPs) are a class of techniques based on the in situ generation of highly reactive and oxidizing radical species which can destroy most of the organic pollutants. AOPs driven by light are found to be the most popular for wastewater treatment due to the abundance of solar light in some regions. The removal of organic contaminants using semiconductor-based photocatalysts has been extensively investigated. However, low charge carrier mobility and rapid electron-hole pair recombination are the common problems that limit the semiconductor-based photocatalysis. Although a large number of alternative systems have been investigated, electron−hole pair separation is still too low in photocatalytic systems. A new concept was introduced recently in which the built-in electric field by ferroelectric, pyroelectric and piezoelectric effects in photocatalytic particles was exploited to enhance the separation of photoinduced charge carriers. Among these new systems that are still under investigation, the use of piezoelectric materials in the photodegradation of pollutants recently drew a lot of attention for environmental remediation. Due to the non-centrosymmetric nature, the piezoelectric materials demonstrate unique catalytic properties as a result of the creation of the built-in electric field by the dipole polarization. This latter provides a driving force for the transport of the photoinduced charge carriers enabling their separation. This review covers the use of piezoelectric materials in photocatalysis and catalysis, especially piezoelectric-catalysis, for environmental remediation. The paper details the fundamentals and basic properties of ferroelectric, pyroelectric and piezoelectric materials. The effect of the built-in electric field in these materials on the photocatalysis/catalysis charge carrier separation is discussed. Possible applications of piezoelectric materials in environmental remediation are reviewed and discussed taking into account several different aspects such as the kinetics of the degradation of the organic pollutants and water splitting. Finally, the current research trends and future prospects of piezocatalysis and piezophotocatalysis are discussed.

Keywords: piezoelectric, pyroelectric, ferroelectric, piezocatalysis, photocatalysis, piezo-photocatalysis, environmental remediation.

2

1. Introduction

the contemporary world is facing the environmental contamination due to the rapid global industrialization leading to the deterioration of the quality of water, air and soil by the accumulated organic and inorganic toxic compounds [1, 2]. These toxic compounds present hazardous properties that affect the ecosystem affecting, in turn, the human health [3, 4]. Today, clean water, air and soil are of great importance for the betterment of the humankind. Among the various environmental remediation methods, the degradation of pollutants by means of photocatalytic semiconductor materials and renewable solar energy has been considered as a promising green technique for the environmental remediation [5, 6].

A semiconductor to be used as a photocatalyst, it should have suitable properties such as appropriate energy positions and gap [7], excellent photostability, low recombination of electron-hole pairs, low cost, and a nontoxic nature [8]. Up to now, a vast number of photocatalytic active semiconductors such as TiO_2, ZnO, ZnS, Fe_2O_3, SnO_2, WO_3, CdS, $CdSe$, CuO, Nb_2O_5 and $SrTiO_3$ [7, 9-12] have been used as photocatalysts and excellent reviews on the environmental remediation by photocatalytic systems have been reported [13-17]. The photocatalytic reactions immensely depend on the generation as well as the separation of e-h$^+$ pairs. These   charge carriers are triggered by the radiation and their efficient separation is vital to participate in the reduction and/or oxidation reactions [18]. Despite many methods have been proposed to enhance the photocatalytic activities further by the band gap tuning, formation of composite semiconductors, anion doping and metal and metal ion implantation, nanostructured morphology maneuvering and introducing defects in the lattice, etc., it is still a challenging task to achieve an efficient charge separation process in photocatalytic systems. In the recent past, there is a keen interest on the use of ferroelectric and piezoelectric materials in photocatalysis to achieve better charge separation. When the piezoelectric materials with ferroelectric properties are employed or coupled with the other photocatalysts, the in-built electric field in the vicinity of piezoelectric material assists the charge separation [19-22]. On the other hand, the "piezophotocatalysis" based on piezoelectric materials without ferroelectric or pyroelectric properties were developed recently and are yet to be explored widely [23-26]. The charge separation process of piezophotocatalysis is resemblance to that of

3

ferroelectric materials wherein the former, the charge separation is achieved by the in-situ generated electric field by the stress while in the latter by the permanent in-built electric field due to the polarization of the dipole [27, 28]. In this review, we report and discuss the recent developments of piezophotocatalysis, especially piezophotocatalysis used for environmental remediation. In the first part, we will discuss the piezoelectric materials including pyroelectric and ferroelectric and their involvement and influence on the photocatalysis/catalysis. In the second part, we will detail the applications and recent progress of piezophotocatalysis/catalysis.

The phenomenon of piezoelectricity or the production of electricity by applying mechanical stress on to a variety of different materials was first observed by the Curie brothers in 1880 [29]. The term "piezoelectricity" is derived from the two Greek words: "*Piezo*" which means to squeeze or press and '*electron*' that refers to amber, a source of electric charge. The piezoelectricity refers to the electricity created when a piezoelectric substance is deformed and hence the piezoelectric effect is a molecular phenomenon which is observed at the macroscopic level [30]. Both organic and inorganic piezoelectric materials can convert mechanical stress into electrical charges, and vice versa. The piezoelectricity origins from the non-centrosymmetric nature of the material, (i.e. crystals not having a center of symmetry in their structure), leads to electric dipoles within the material. In most crystals, the unit cell is symmetrical but not in piezoelectric crystals. Despite their asymmetric arrangement of atoms in the lattice, piezoelectric crystals are electrically neutral as a result of canceling out a positive charge by a neighboring negative charge. However, if a piezoelectric crystal is subjected to stress by squeezing or stretching, the atoms are displaced from their original position gaining a net electrical charge in the whole crystal and hence net positive and negative charges appear on the opposite and outer faces of the crystal i.e wurtzite ZnO [31, 32]. The hexagonal wurtzite ZnO crystal structure lacks the center symmetry in which Zn^{2+} cations and O^{2-} anions are tetrahedrally coordinated and the centers of the positive ions and negatives ions overlap with each other and do not show spontaneous polarization. When a stress is exerted on the unit cell, the original atomic positions of O^{2-} anions and Zn^{2+} cations are relatively displaced and that would lead to gaining of a dipole moment in the unit cell

4

(Figure 1a). Hence, a crystal gains a piezoelectric potential due to the collective induced polarization of charges in whole unit cells in the crystal (Figure 1b) which is the piezoelectric potential (piezopotential) [33].
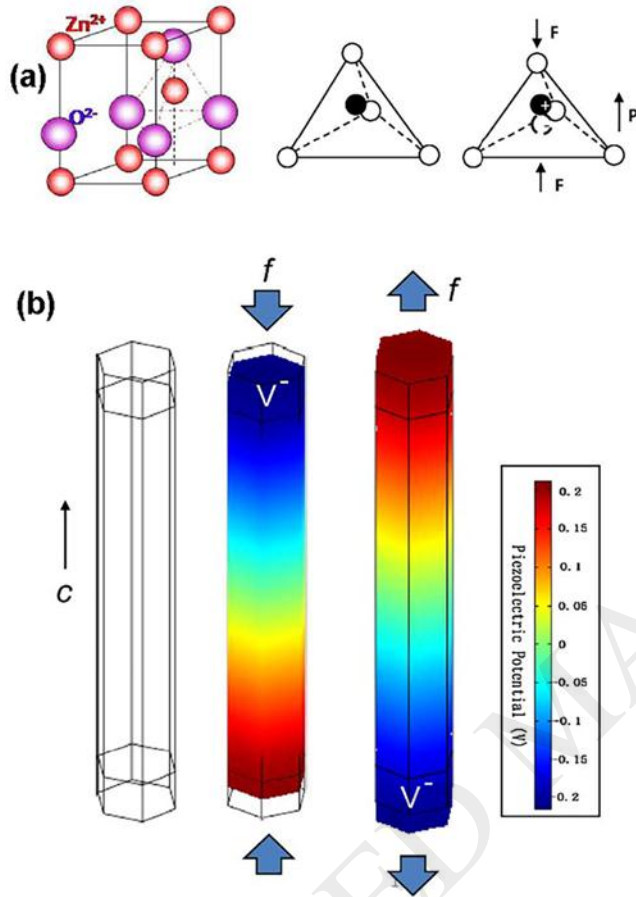

Figure 1. Piezopotential in wurtzite crystal: (a) Atomic model of the wurtzite-structured ZnO. Reproduced with permission [34] (b) Numerical calculation of the piezoelectric potential distribution in a ZnO nanowire under axial strain. The growth direction of the nanowire is c-axis. The dimensions of the nanowire are $L = 600$ nm and $a = 25$ nm; the external force is $fy = 80$ nN. Reproduced with permission [32].

The materials that possess piezoelectric properties are subcategorized into ferroelectrics, pyroelectrics and piezoelectrics [35, 36]. The understanding of the symmetry of crystalline structure is important for the understanding of the origin of the piezoelectricity and hence the symmetry of element is briefly discussed in the following section. Out of the 32 crystal point groups, 21 are non-centrosymmetric and among them, 20 point groups exhibit the piezoelectric effect. Again, among these 20 non-centrosymmetric point groups, 10 belong to polar crystals i.e. crystals that possess a unique polar axis (an axis showing different

properties at the two ends) (Figure 2) [37, 38]. The spontaneous polarization can occur only in materials that possess a unique polar axis and these polar crystals can be spontaneously polarized. If an electric charge is developed on the faces of the crystal perpendicular to the polar axis upon the change in temperature on these crystals, they are pyroelectric e.g., ZnO, $(CH_2CF_2)_n$ and $Pb(Zr, Ti)O_3$. If the polarization along the polar axis of the polar crystals can be reversed by reversing the polarity of the electric field, such crystals are called ferroelectric (spontaneously polarized materials with reversible polarization). Hence, by default, all ferroelectric materials are simultaneously pyroelectric and piezoelectric (Figure 2). Similarly, all pyroelectric materials are piezoelectric, but only some piezoelectric materials (those whose symmetry belongs to polar groups) are pyroelectric such as AlN and GaN [39, 40] (Figure 2).
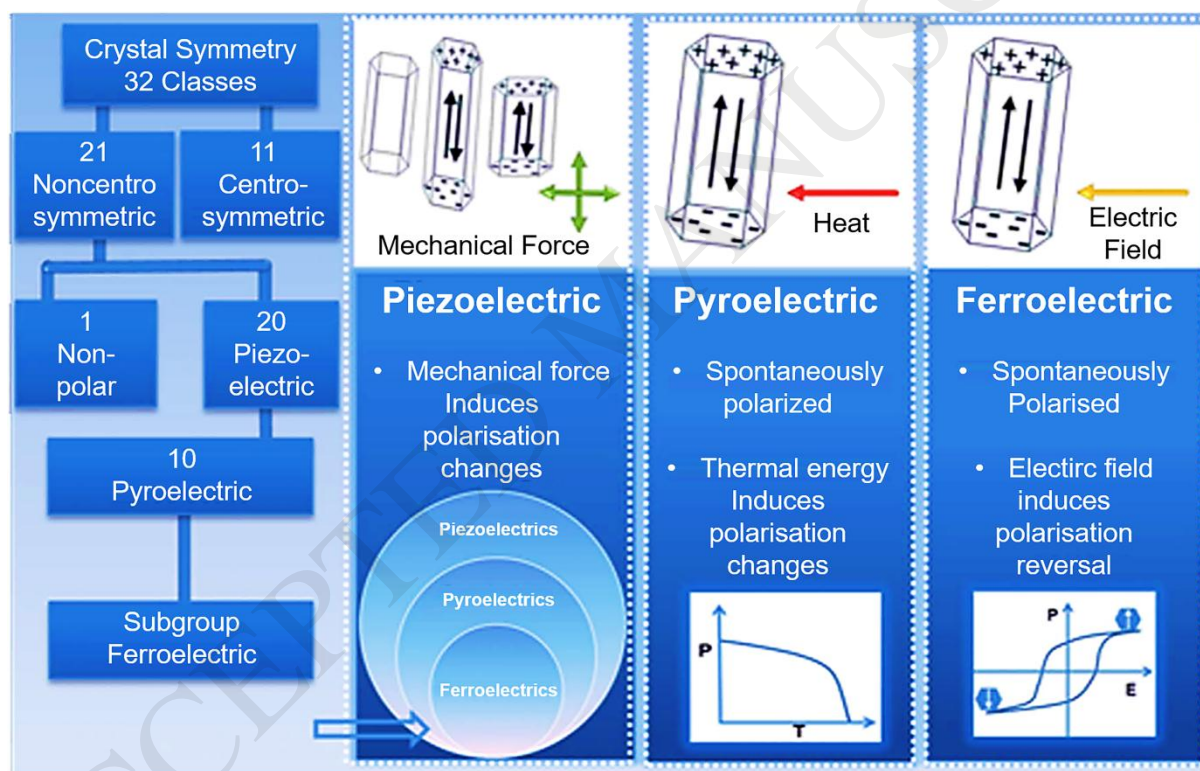

Figure 2. The relationship between piezoelectric, pyroelectric and ferroelectric. Reproduced with permission [41].

No matter the origin (mechanical, thermal or spontaneously), the in-built electric field in materials affects the reactions taking place on their surfaces [42-47]. In a non-ferroelectric/piezoelectric semiconductor (i.e. non-polar domain, e.g. TiO_2, Figure 3a,i), free carriers are moved to the interface due to differences in local chemical potential that

6

result in band bending when in contact with an ionic solution. Figure 3a(ii) shows that in a

ferroelectric/piezoelectric semiconductor, a spontaneous internal electric field can be

generated due to the polarization of charges. These polarized charges are neutralized

producing a depolarization field either by the flow of free charges within the crystal or by the

absorption of ions on the polarized crystal surface by the surrounding medium [48-50]. The

surface at which the polarization produces a positive potential is labeled as the C^+ domain and

the surface where the polarization produces a negative potential is labeled as the C^- domain.

(Figure 3a,iii)   As illustrated in Figure 3b, in a positive surface (C^+ domain), a potential is

dropped across the domain, such that the surface is at a lower potential than the bulk causing

downward bending at the C^+ domain. Similarly, in a negative surface (C^- domain), a potential

is gained across the domain, such that the surface is at a higher potential than the bulk causing

upward bending at the C^- domain leading to the accumulation of electrons and holes at C^+ and

C^- faces respectively. Thus, the internal electric field of a ferroelectric material exhibits a

spontaneous polarization and acts like an internal p–n junction. The strength of the internal

electric field determines the band bending at the interface. Henceforth, with the appropriate

control of the built-in-fields, photogenerated electrons and holes can be driven to the different

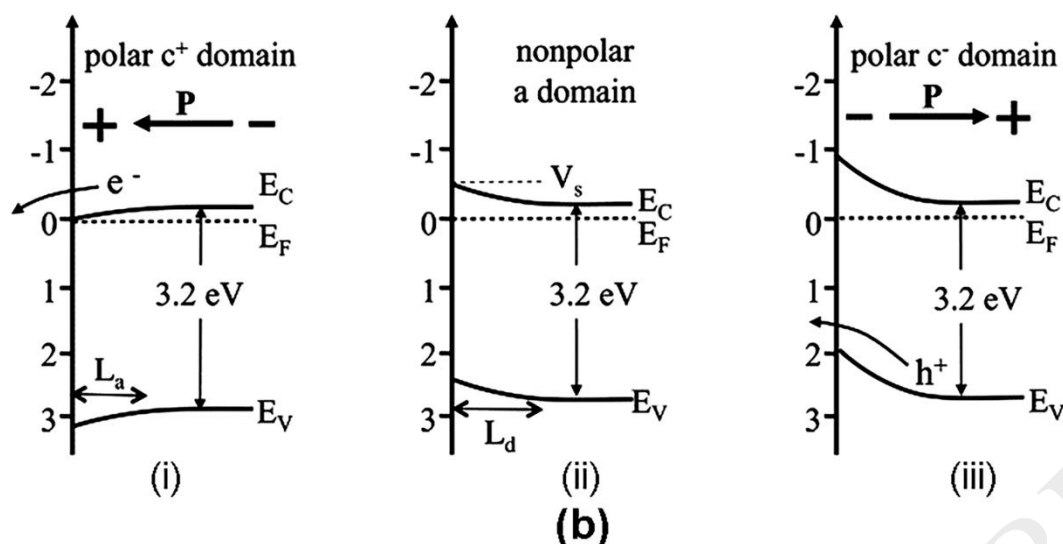interfaces of the crystal to achieve efficient charge separation.
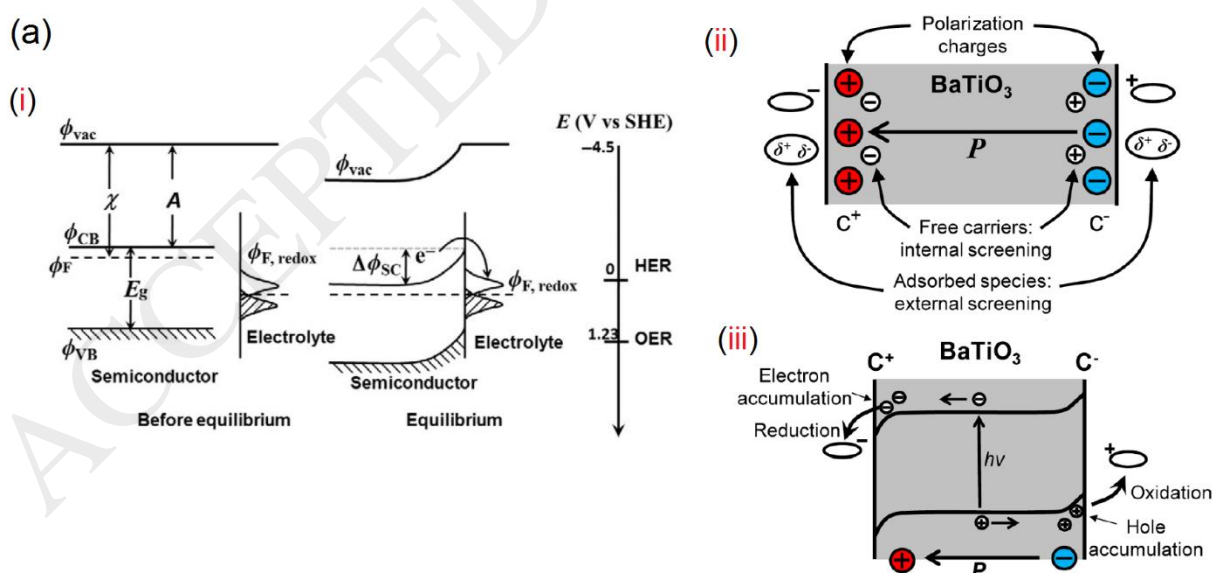
Figure 3. Band diagram of semiconductor/electrolyte interfaces (a, i). (The drawings are based on an n-type semiconductor. χ and A are the semiconductor work function and electron affinity, respectively. The band bending is $\Delta\phi SC\frac{1}{4}\phi F,SC\_\phi F,redox$ (or $\phi F,M$)) Schematic of a ferroelectric material showing (a, ii) internal polarization and screening mechanism, (a,iii) the effect of free carrier reorganization on band structure and photo-excited carrier. Reproduced with permission [51], (b) Energy level diagrams for $BaTiO_3$ in aqueous solution, without illumination. The energies on the vertical axes are on the standard hydrogen electrode scale. E_v is the valence band edge, E_F is the Fermi level, E_C is the conduction band edge, Vs is the surface potential, L_d is the width of the space charge layer in depletion, and L_a is the width of the space charge layer in accumulation. Band bending (i) for a c+ domain, (ii) for a domain, and (c) for a c^- domain. Reproduced with permission [50, 52].

Figure 4 shows that in the ferroelectric materials the electric field is generated spontaneously while in pyroelectric and piezoelectric materials it is generated under the thermal effect and mechanical energy respectively. One of the major challenges in photocatalysis is to achieve an efficient charge separation hindering their recombination. Therefore, the in-built electric field in piezo/pyro/ferroelectric semiconductors provides a practical strategy to improve the photocatalytic activity by effective separation of the photo-excited carriers by the internal polarization. In the following section, the piezoelectric field and its influence on the catalytic and photocatalytic environmental remediation are discussed.

In general, under the influence of the piezoelectric effect, the free carriers in the materials are separated as shown in Figure 1, 3a (ii) and 3a (iii). Once these charges are accumulated at the interface, they can generate free radicals reacting with the adsorbed molecules.
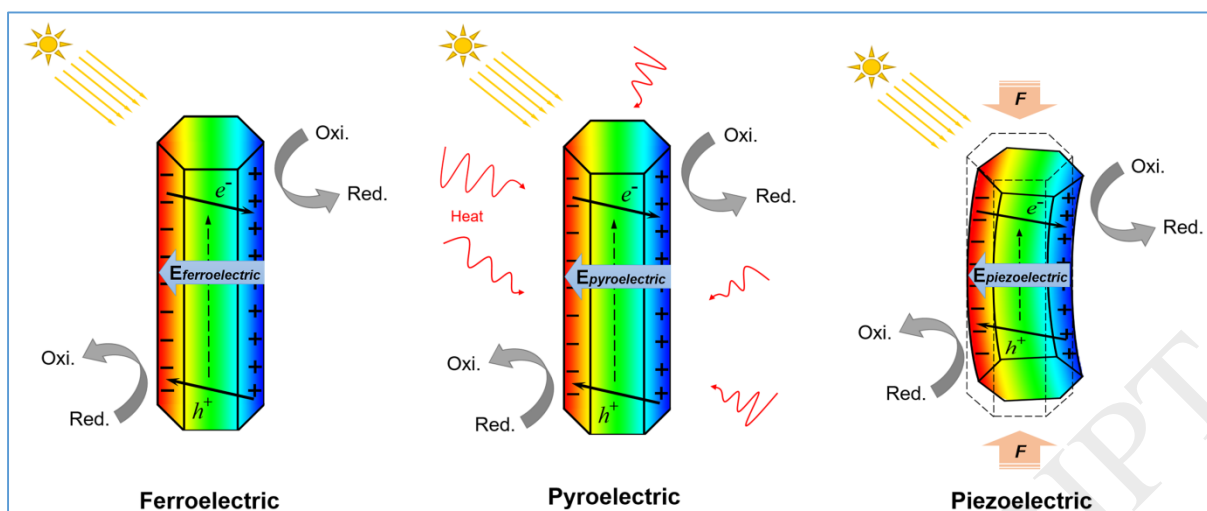
Figure 4. Schematic understanding of free carrier reorganization and photo-excited carrier separation in ferroelectric, pyroelectric and piezoelectric materials under the influence of ferroelectric [spontaneous polaraization], pyroelectric [thermal] and piezoelectric [mechanical force, F) effects respectively.

2. Piezoelectric materials, photoelectric effects and their applications

The presence of the piezopotential in a crystal has created few new research fields where the piezoelectric effect in materials can be used to convert mechanical energy into electrical energy, or vice versa [53, 54]. Starr et al. reported the fundamental processes occurring at the surface of the piezoelectric materials during piezoelectric-potential driven electrochemical H_2 evolution reaction [49, 53]. The piezoelectric polarization and internal electric field inside semiconductor nanostructures have been applied in piezoelectric nanogenerators optoelectronics, sensors, piezoelectric transducers, transparent conductor and nanogenerators successfully [55-60]. However, it has not been exploited fully in catalysis/photocatalysis. In the following section, we expose the recent progress and applications of the piezoelectric materials, especially in photocatalytic environmental remediation. The quartz and Tourmaline are natural piezoelectric crystals [61-63] while $BaTiO_3$ [64], $PbTiO_3$ [65], $Pb(Zr,Ti)O_3$–PZT [66-69], $KNbO_3$ [70], $LiNbO_3$ [71, 72], $LiTaO_3$ [73] are manmade piezoelectric ceramics and polyvinylidene fluoride – PVDF, polyparaxylene, poly-bis(chloromethyl)oxetane, aromatic polyamides, polysulfone, polyvinyl fluoride, are manmade piezoelectric polymers [74, 75].

2.1. Piezoelectric and catalysis

The piezoelectric in chemical catalysis (PZEC) or the direct conversion of mechanical

energy into chemical energy, was first reported in 2010 by Hong et al. [76]. In PZEC, the mechanical stress induced localized-polarization charges can be effectively utilized to control the carrier generation, separation, transport, and recombination by modifying the local electrical field distribution at the vicinity of the metal-semiconductor interface which depends on the electronic states of the piezoelectric materials and the reaction medium [77-80]. The piezocatalytic process strongly resembles to that of the conventional electrocatalytic process wherein the former the electrical potential that drives the electron is in-built while in the latter it is an external power source. Starr et al. discussed the theoretical analyses of the piezocatalysis process of piezoelectric semiconductor in detail [44, 53]. If the strained induced potential in piezoelectric materials is higher than 3 volts, (versus standard hydrogen electrode (SHE)), then the charge carriers in the piezoelectric materials can participate in the reduction or oxidation reactions.

Wu et al., explained more explicitly the piezocatalytic process by using $BaTiO_3$ nanowires as a model piezoelectric material [81, 82]. In the absence of piezoelectric polarization, no charges are generated in $BaTiO_3$ except free electrons and holes in semiconductors due to thermally activated charges at temperatures above 0 K. As shown in Figure 5a, even in the absence of piezoelectric polarization (before applying mechanical stress) the electrons in the CB of BTO can reduce the adsorbed O_2 molecules to $O_2{}^{\bullet-}$ radicals. This was attributed to the conduction band (CB) energy level of BTO (-0.83 V vs. the normal hydrogen electrode, NHE) [83] which is more negative than the standard redox potential of $O_2{}^{-}\bullet/O_2$ (-0.33 V vs. NHE) [71]. The same is true for the valence band (VB) of BTO ($+2.31$ V vs. NHE) [83], as the energy level of VB of BTO is more positive than the standard redox potential of $\cdot-$OH/OH ($+1.9$ V vs. NHE) [82, 83] holes in the VB can oxidize the $-$OH to $^{\bullet}$OH radicals. However, as the concentration of free charges in a perfect BTO crystal is very low at thermal equilibrium in the absence of piezoelectric polarization, no redox reaction was observed without an external force (Figure 5a). However, upon induced stress on BTO, the created piezoelectric potential gradient within the crystal (depending on the piezoelectric strength) [84] attracts these free charges towards opposite directions of the crystal surfaces and react with dissolved oxygen and hydroxyl to form $O_2{}^{\bullet-}$ and $^{\bullet}$OH radicals (Figure 5b) [51,

10

85, 86]. However, the piezoelectric potential decreases to zero when the accumulated external screening charges at the surface are high enough to balance the polarization charges and consequently the driving force for charge transfer will be suppressed and the redox reactions will be retarded by the new potential equilibrium (Figure 5c). Again, the new potential equilibrium in BTO will break down by the falling pressure leading to reverse the charge transfer and new redox reactions (Figure 5d).
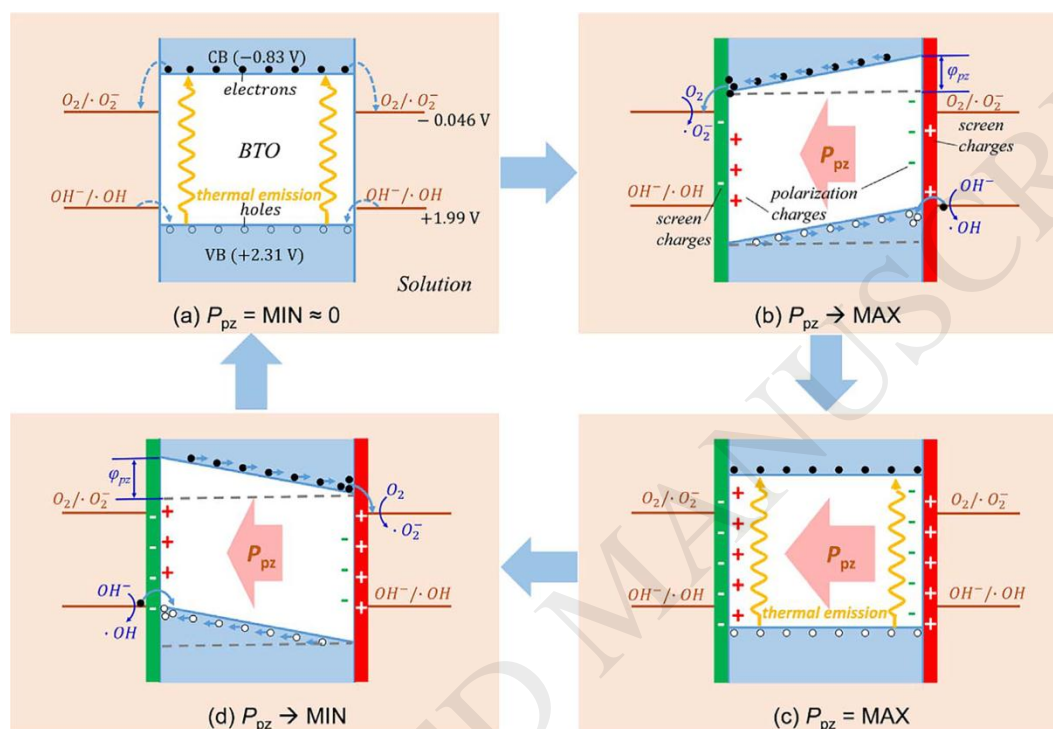

Figure 5. Principle scheme of the piezocatalysis, which contains band tilting and surface reaction during the ultrasonic vibration: (a) No obvious degradation can be observed without piezoelectric polarization and piezoelectric potential; (b) Free electrons and holes within the BTO catalyst are attracted in opposite directions and the band are tilted by the piezoelectric potential; (c) Piezoelectric potential decreased to zero due to the new balance between polarization charges and screen charges; (d) The decrease in polarization upon falling pressure will break the potential equilibrium again, leading to reverse charge transfer and new redox reactions disappear. Reproduced with permission [81].

As explained earlier, due to the piezoelectric effect, the charges are accumulated at the CB and the VB of the semiconductor material leading to the shift in the CB and VB positions. Hence, the shift in the CB and VB positions due to the high piezoelectric potential has been simulated by FEM (finite element method) [81]. Starr et al. showed that the piezoelectric semiconductors should possess a high piezoelectric coefficient, a low electrical conductivity and the electrical permittivity needs to be optimized to exhibit a high electrochemical activity

[53]. Several applications of piezoelectric materials in catalysis/photocatalysis have been reported after the first report on PZEC. In the following section, these applications will be described in details.

2.2 Piezocatalytic degradation of organic pollutants

After their first report on water splitting on piezoelectric ZnO microfibers and BaTiO₃ microdendrites by stress-induced charge generation [76], Hong et al. reported on the degradation of an organic dye, acid orange (AO7) on piezoelectric BaTiO₃ microdendrites by harvesting mechanical energy [87]. Upon applying a strain on piezoelectric BaTiO₃ microdendrites, a nonzero dipole moment in the crystal lattice was noticed due to the variation of the relative Ti-O positions leading to strain-induced charge generation on the surface of the BaTiO₃ microdendrites (Figure 5). As shown in Figure 6, a stress induced by bending produces free negative charges on the tensile face and positive charges on the compressive face and the free charges in respective sides take part in the reduction and oxidation reactions respectively. The important point here is that the developed free charges must have higher potential than the standard redox potential of any redox reaction that is to say more than 1.23 eV in the case of water splitting. Moreover, any charge potential lower than the redox potential would not induce the redox reaction (Figure 6).
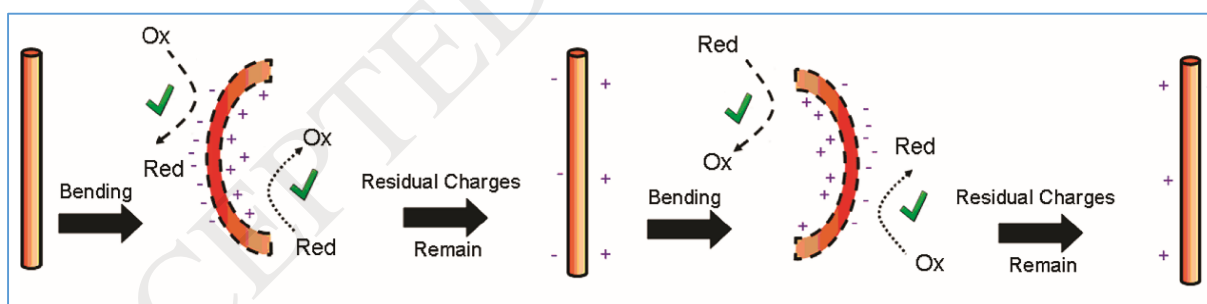

Figure 6: Schematic diagrams showing the charges developed on fiber surface through bending with ultrasonic vibration. (Procedures of piezoelectrochemical reactions through fiber bending, showing that only the induced potential greater than that of standard reduction potential of water will trigger the reaction. Reproduced with permission [76].

It was shown that the pH of the reaction medium plays a less significant role on the piezocatalytic degradation of AO7 with piezoelectric BaTiO₃. Similarly, Xu et al., showed that up to ~ 80% AO7 discoloration (5 mM) was achieved on piezoelectric ZnO nanorods [88]. By

increasing the mass of the catalyst from 25 mg to 35 mg, a negligible decrease in AO7 degradation was observed. Further research is needed to verify the interdependence between the piezocatalytic activity and the mass of the piezoelectric catalyst. A similar less dependence of piezoelectrocataly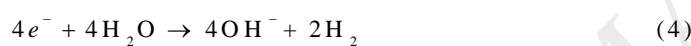tic activity on the mass of the catalyst has been noted with the piezoelectric $Pb(Zr_{0.52}Ti_{0.48})O_3$ fibers for the degradation of AO7. The observed slight decrease in catalytic activity was attributed to the quenching of the generated electric charges [89]. The generation of free charges and their participation in redox reactions in piezocatalytic process were given in reactions (1) to (12) as previously reported [87].

$$BaTiO_3 + vibration \rightarrow BaTiO_3\ (e^- + h^+) \tag{1}$$
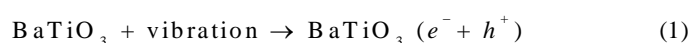
Anode (negatively charged sides of the $BaTiO_3$):

$$4e^- + 4H_2O \rightarrow 4OH^- + 4H^\bullet \tag{2}$$

$$4H^\bullet \rightarrow 2H_2 \tag{3}$$

Overall:

$$4e^- + 4H_2O \rightarrow 4OH^- + 2H_2 \tag{4}$$
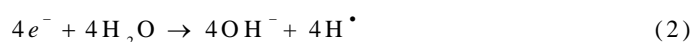
Cathode (positively charged sides of the $BaTiO_3$):

$$4OH^- \rightarrow 4e^- + 4^\bullet OH \tag{5}$$

$$2(^\bullet OH + {}^\bullet OH) \rightarrow 2H_2O + 2O^\bullet \tag{6}$$

$$2O^\bullet \rightarrow O_2 \tag{7}$$

Overall:

$$4OH^- \rightarrow 4e^- + 2H_2O + O_2 \tag{8}$$
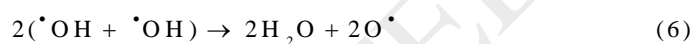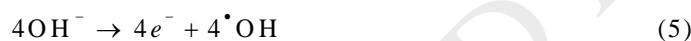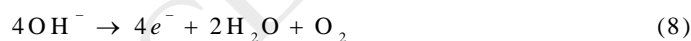
Net reaction of water decomposition:

Dye decomposition:

$$^\bullet OH + dye \rightarrow degradation\ products\ of\ dye \tag{10}$$

$$e^- + dye \rightarrow degradation\ products\ of\ dye \tag{11}$$

$$h^+ + dye \rightarrow degradation\ products\ of\ dye \tag{12}$$
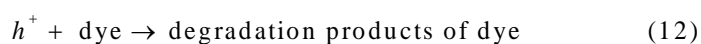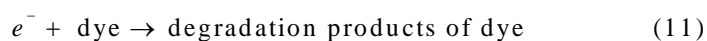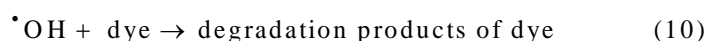
Carbon nanotubes (single or multiple walls, SWCNTs and MWCNTs) have been extensively used as a scaffold for transporting the photogenerated charges in photocatalysis [90-92]. Li et al. embedded the piezoelectric ZnO nanorods and nanoparticles on MWCNT network to accelerate the charge transport and separation. They tested the piezoelectric degradation of Methylene Blue (MB) [93, 94]. In MWCNTs-ZnO catalyst, the contact between CNTs and ZnO is a Schottky contact (the work functions of MWCNT and ZnO are 5.2 and 4.5 eV respectively) in which MWCNTs act as the metal and ZnO as the semiconductor. The piezoelectrically generated electrons in ZnO nanostructures flow to the MWCNTs only when the compressed side of the ZnO nanostructures is contacted with MWCNTs. This was attributed to the formation of a positively biased Schottky diode. However, when MWCNTs nanostructures are contacted with the stretched ZnO surface, the electrons are accumulated in ZnO due to the formation of a reverse biased Schottky diode. The electrons that are created in ZnO nanostructures due to piezoelectric effect can transfer to the MWCNTs (which act as molecular wires) while the holes stay in ZnO enhancing the piezocatalytic activity (enhanced charge separation).

On the other hand, $Pb(Zr_{0.52}Ti_{0.48})O_3$ (PZT) fibers are excellent piezoelectric material that exhibits better piezoelectric effect than the piezoelectric ZnO nanostructures [95, 96]. Lin et al. investigated the piezocatalytic effect of PZT fibers for the degradation of AO7 dye and noted a high piezocatalytic effect [89]. The reported AO7 degradation rate on PZT fibers by Lin et al was found to be higher than that of ZnO nanostructures [88] which could be due to the fact that PZT fibers were easily bent and hence a large amount of electrical charge was generated by the highly piezo-active PZT material.

Similarly, MoS_2 and $MoSe_2$ are another interesting non-symmetric transition metal dichalcogenides (TMDC) that have been investigated for piezoelectric degradation of pollutants due to their superior piezoelectricity in their single layer and/or odd layered structure. Due to their weak piezoelectric response in the MoS_2 structure [97], the piezocatalytic activity of the commercial MoS_2 bulk sheets was still very low. However, by piezo-response force microscopy (PFM) analysis, Wu et al discovered that the MoS_2 nanoflowers (NFs) have a high piezoelectric potential on the edge sites of the single and

14

few-layer MoS$_2$ NFs and hence high piezocatalytic effect for the degradation of the organic dyes [98]. The piezocatalytic activity of MoS$_2$ NF has been attributed to the creation of a significant piezopotential due to the presence of an odd number of layers that exhibited a non-centrosymmetric structure. This structure would lead to the release of an electric charge by separating the free electrons (majority carriers) and holes (minority carriers) under the mechanical-stress assistance. The reported electron mobility and electron concentration of MoS$_2$ NFs ≈ 12.9 cm$^2 \cdot$V$^{-1} \cdot$s^{-1} and 4.04×10^{15} cm^{-3} respectively are relatively high and hence the abundant odd number of layers present in MoS$_2$ could create a significant piezoelectric potential. Hence, the high piezocatalytic degradation activity of the MoS$_2$ NFs is mainly due to the enhanced separation of a large number of free carriers in the catalysts under the enhanced piezoelectric potential caused by the mechanical stress. An even higher piezophotocatalytic activity was observed with the single-layer and few-layered MoSe$_2$ nanoflowers for removing rhodamine B (RhB) under the sonication. The degradation rate of RB on MoSe$_2$ nanoflowers is much faster than the MoS$_2$ nanoflowers [99] due to the high density of carrier concentration and the higher piezoelectric properties [100]. The measured carrier concentration and electron mobility of the MoSe$_2$ nanoflowers $\sim -3.803 \times 10^{17}$ cm^{-3} and ~ 20 cm$^2 \cdot$V$^{-1} \cdot$s^{-1} respectively, which are higher than that of MoS$_2$ nanoflowers due to high native selenium vacancies in MoSe$_2$ nanoflowers [27, 101]. The generation of piezopotential and piezocatalytic activity in MoSe$_2$ is similar to that of MoS$_2$ where non-centrosymmetric single and/or few layered MoSe$_2$ creates a spontaneous polarization under mechanical stress that would lead to the flow of free carriers in the opposite direction leading to highly reactive $\cdot$OH and O$_2 \cdot^-$ radicals.

In a recent report, the piezocatalytic activity of multiferroic BiFeO$_3$ material that exhibits a large spontaneous polarization in excess of 100 μC$\cdot$cm^{-2} and a strong piezoelectric effect piezoelectric coefficient (d_{33}) of ~ 70 pm$\cdot$V^{-1} [102] was tested for the degradation of RhB dye by You et al. [103]. When multiferroic BiFeO$_3$ are subjected to mechanical vibration, a large number of positive and negative charges are generated on the BiFeO$_3$ surfaces due to strong piezoelectric effect and the strongly oxidative $\cdot$OH radicals generated by the reaction of OH$^-$ and h$^+$ leading to dye decomposition. The piezoelectric catalytic degradation processes

described so far assumed that the piezoelectric enhanced charges participate in the redox reactions and accordingly degradation mechanisms have been proposed. However, the generated charges are not free-state and cannot migrate [104] as they are formed by the relative displacement of positive and negative charges under the mechanical stress (still under bound state) and would not involve in the degradation process. On the other hand, if free charge carriers are present due to defects in these materials, they can be effectively separated under the influence of piezoelectric potential generated under stress and could involve in redox reactions. Hence the possible scenario would be that the reported piezoelectric materials possess free carrier charges due to the formation of defect states during their synthesis and these free carrier charges actively separate and participate for redox reactions under the piezoelectric potential exerted by the mechanical stress.

It is known that due to flexible nature of 1D and 2D nanomaterials than the 3D materials, 1D and 2D nanomaterials can be bent easily under mechanical forces and hence higher piezocatalytic performances are generally expected with one or two dimensions piezoelectric materials. Based on this assumption, the piezoelectric catalytic research had been mainly focused only on 1-D or 2-D piezoelectric materials. However, in a recent study, Feng et al, scrutinized the relationship between the deformation and the piezoelectric catalytic performance by using spherical piezoelectric lead zirconate titanate (PZT) instead of one or two-dimensional piezoelectric structures to access the explicit role played by 1D and 2-D structures in the piezocatalytic process [105]. Generally, spherical PZT particles with a diameter ranging from 0.2 μm to 2.5 μm demonstrated the piezocatalytic activities. Piezocatalytic activity indicates that the degradation efficiency of RhB gradually increased from 10% (at 200 rpm stirring speed) to 37% (at 900 rpm stirring speed) with the spherical PZT as shown in Figure 7a. This was attributed to a stronger built-in electric field in PZT as a result of the increased stress from stirring at higher rpm. In the same study, Feng et al used three different types of PZTs such as Zr-rich PZT-1 doped with Bismuth ferric (BF) at high temperature, PZT-2/undoped (prepared by high-temperature solid phase method) and PZT-3/undoped (prepared by hydrothermal method). It was shown that despite PZT-1, PZT-2 and PZT-3 having the same crystal structure, the piezocatalytic activity of doped PZT-1 (0.36

16

m^2/g) and undoped PZT-2 (1.0 m^2/g) were 30 and 7% respectively while undoped PZT-3 (7.7 m^2/g) has no piezocatalytic effect. Feng at al., argued that the absence of free charges in PZT-3 was the reason for the absence of piezocataltyic degradation of RhB dye on PZT-3. Hence, they concluded that the piezoelectric potential induced from the polarized charges could not participate directly in the redox process. Further, the piezoelectric materials should contain free charges (by narrow band gap semiconductor or defect doping) in order to be piezocatalytic active and these free charges are separated under the influence of piezoelectric potential generated under stress (Figure 7b).
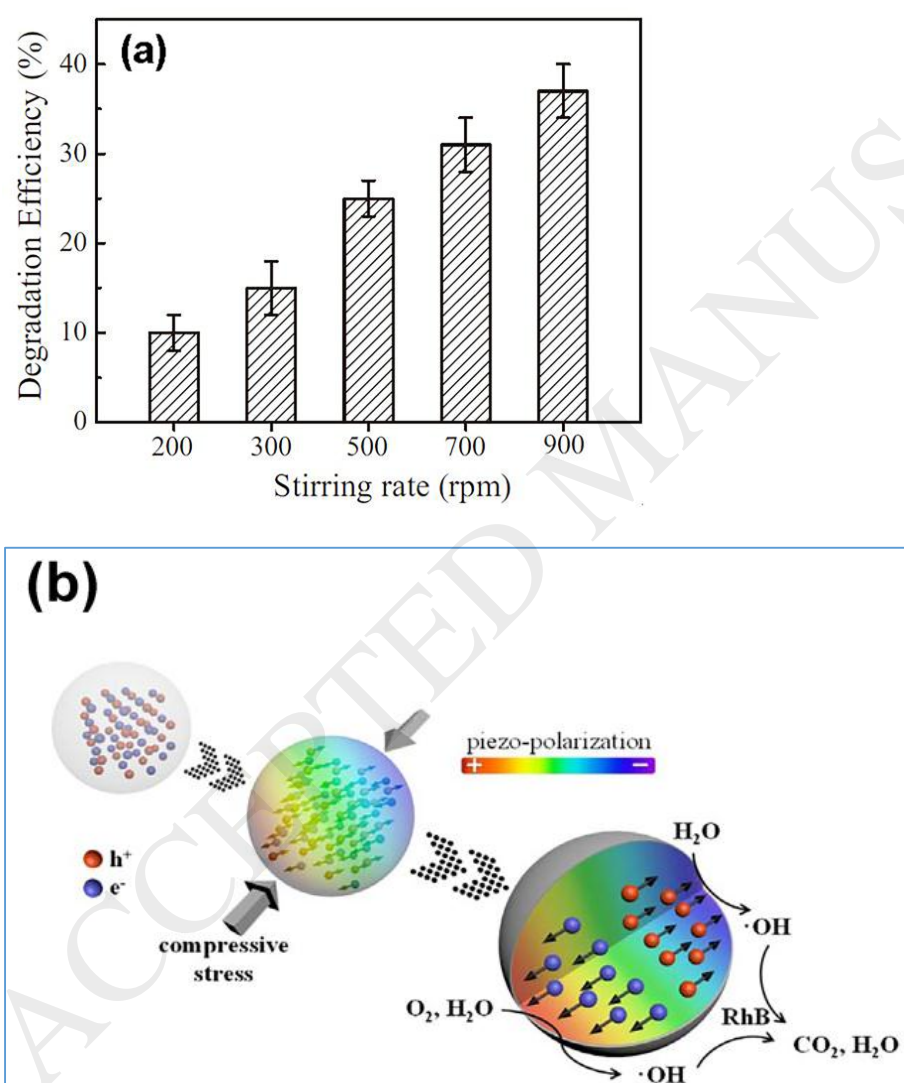

Figure 7. (a) Piezo-catalytic degradation of RhB at different stirring rates (reaction time = 30 min). Reaction conditions: RhB solution (10 ppm), PZT-1 concentration (5 g/L), reaction temperature = 293K. (b) Proposed reaction mechanisms of piezo-catalysis of PZT. Reproduced with permission [105].

The presence of free charges in these materials is essential to induce the piezocatalytic

activity as previously reported [98, 105]. Subsequently,   strong piezoelectric properties and a strong piezocatalysis can be observed on 3D piezoelectric materials. Similarly, Wu et al. clearly demonstrated that the intrinsic charge carrier density and not the piezoelectric charges in piezoelectric crystallites is the key factor in charge transfer in the piezocatalysis process and hence piezocatalytic process can be enhanced through regulating the concentration of charge carriers [81]. As mentioned previously, 1-D and 2D piezoelectric nanostructures can advantageously combine/bend generating a stronger piezoelectric field. However, further investigations are needed to explain the explicit role or the necessity of 1-D and 2D structures in piezocatalysis.

The literature search indicated that the most of the highly piezoelectric materials contain toxic Pb. In order to avoid the toxic Pb, leadless piezoelectric materials such as piezoelectric $MoSe_2$ [99], MoS_2 [98], $BiFeO_3$ [103] and $BaTiO_3$ [81, 106] have been tested as piezocatalysis. Among them, $BaTiO_3$ was shown as a good candidate that can be synthesized by various methods [107, 108]. Tetragonal $BaTiO_3$ nano/micrometer-sized particles were prepared by Lan et al. and tested for the piezocatalytic degradation of 4-chlorophenol (4-CP) [106]. In general, a majority of the piezocatalytic activities are assessed mainly on their ability to degrade organic dyes. Lan et al. used 4-chlorophenol (4-CP) which is a typical toxic chlorinated compound used as a model of a non-dye pollution. Piezocatalytic degradation of 4-CP was carried out on hydrothermally synthesized tetragonal $BaTiO_3$ nano/micrometer-sized particles [106]. The observed 4-CP degradation efficiency with t-$BaTiO_3$ mediated piezocatalysis is 71.1%, which is comparable to that of common organic dye degradation efficiencies with common piezoelectric materials [88, 95]. The piezocatalytic 4-CP degradation mechanism is the same as on other similar piezoelectric materials where $^{\bullet}OH$ and $O_2^{-\bullet}$ radicals generated by the piezoelectric effect leading to the removal of 4-CP. Similar to $BaTiO_3$, leadless piezoelectric $Bi_4Ti_3O_{12}$ is a multiferroic material that produces piezoelectric charges on its surface when subjected to mechanical vibration. Especially, piezoelectric multiferroic materials are important in piezocatalysis as they easily undergo bending/deformation to produce the piezoelectric potential. Tu et al. used diverse morphologies of piezoelectric $Bi_4Ti_3O_{12}$ synthesized by hydrothermal (nanorods,

18

slice-assembled microspheres, nest-like hollow microspheres, and cube assembly) and sol-gel methods (SG-$Bi_4Ti_3O_{12}$). They studied the impact of the $Bi_4Ti_3O_{12}$ morphology and surface area on its piezoelectric catalysis [109]. The methyl Orange (MO) dye was degraded at almost similar rates on both hydrothermally synthesized $Bi_4Ti_3O_{12}$ and SG-$Bi_4Ti_3O_{12}$ despite morphologies and specific areas of nanosheet $Bi_4Ti_3O_{12}$ and SG-$Bi_4Ti_3O_{12}$ were greatly different. They concluded that the morphology and the surface area have little impact on the catalyst piezoelectric activity.

In an attempt to enhance the piezocatalytic degradation of pollutants, the piezocatalytic process is further expanded by coupling of traditional piezocatalytic effect with the Fenton reaction by adding ferric ions into the reaction medium of piezoelectric materials. Lv et al., combined $BaTiO_3$ microcrystals with ferrous ions to achieve 93.4% AO7 dye degradation efficiency. However, this efficiency was similar in the absence and presence of ferrous ions [110]. Similarly, by adding 4 mg.L^{-1} ferrous ions into the $BaTiO_3$ reaction medium, the degradation efficiencies of phenol and 4-chlorophenol increased by 16.9% and 7.8%, respectively. It has been reported that the H_2O_2 is formed on the piezoelectric $BaTiO_3$ under sonication and the enhancement effect of ferrous ions originated from an H_2O_2-related Fenton reaction (reaction 13) that generates active $\cdot$OH radicals which can oxidize the organic pollutants efficiently as previously reported [111, 112]. However, further investigation has to be carried out to confirm the piezoelectric effect on the Fenton reaction.

$$H_2O_2 + Fe^{2+} \rightarrow \cdot OH + OH^- + Fe^{3+} \qquad (13)$$

The research on the use of piezoelectric materials for the environmental remediation by piezoelectric catalysis is surging and several novel piezoelectric materials have been prepared. However, a real comparison of piezocatalytic degradation activities of different piezoelectric materials cannot be compared accurately owing to the fact that the piezocatalytic activities of these materials have been reported with respect to reaction products or the initial concentration. For an accurate comparison of piezocatalytic activities of different piezoelectric materials, one should compare the piezoelectric properties of different materials.

However, piezoelectric properties of the majority of these materials have not been reported and hence major information is lacking. Similarly, it has been proposed that $^{\cdot}OH$ and $O_2^{-\cdot}$ radicals are formed during piezocatalysis, a firm evidence for   the formation of $^{\cdot}OH$ radicals has not been reported and hence a detail investigation is imperative to draw a valid piezocatalytic mechanism.

2.3 Piezophotocatalytic materials and organic pollutants degradation

The semiconductor-based photocatalysts have been widely investigated for environmental remediation [5, 113, 114]. In photocatalysis, electron-hole pairs are generated in the semiconductor nanostructures by the excitation of electrons from the valence band to the conduction band by absorbing light with the certain energy. The photogenerated carriers participate in the oxidation and reduction reactions after migrate to the catalyst surface. During this process, the recombination of the photogenerated electrons/holes can lower down the photocatalytic activity. The charge carrier generation as well as their transport and recombination have to be precisely controlled in order to enhance the photocatalytic activity. Many attempts to optimize the photocatalytic activity have been reported in recent reviews by Fagan et al. [115] and Dong et al. [116].

In the previous sections, we have briefed the use of piezoelectric materials in piezocatalysis.   Similarly, when a semiconducting piezoelectric material is coupled with photons excitation, the coupling effects of piezoelectric, semiconductor and photonic properties in the noncentrosymmetric semiconductor material is known as the piezo-phototronic effect [47, 117, 118]. In piezophotoronics, semiconductor materials (presenting optical and piezoelectric properties), the piezoelectricity is coupled with photonic properties leading to control the charge carrier generation, transport, separation and recombination at the metal-semiconductor junction improving the performance of optoelectronic devices [34, 119]. The piezoelectric field of piezoelectric materials has been recently coupled with the photocatalytic process to optimize the photocatalytic activity. In the following section, we report recent progress in the field of piezoelectric-photocatalysis and their applications.

The piezo-phototronic effect can be used to tune/control the charge separation, transport and recombination at the semiconductor/piezoelectric junction in piezophotocatalysis. The piezoelectric effect on the photocatalytic activity has been tested with Ag_2O/tetrapod-ZnO [120] and Ag_2O/$BaTiO_3$ [121] under ultrasonic/UV exposure for the degradation of organic pollutants. Sun et al. used Ag_2O/tetrapod-ZnO nanostructures and under UV and ultrasonic exposure, more than 99% of MB (5 mg/L) degradation was attained within 120 s. Also, other common dyes such as Rh B, Rh 6G and MO were degraded within 180 s (99%), 150 s (97%) and 240 s (92.3%), respectively under the similar piezophotocatalytic conditions [120]. Enhanced catalytic activity was assigned to both the built-in-electric field due to the formation of p-n junction between Ag_2O-ZnO [122-124] and to the piezoelectric field of ZnO nanostructures that enable rapid separation of excited charges. The fast dye degradation was attributed to the generation of a high piezoelectric filed in the Ag_2O/T-ZnO nanostructures under light irradiation and high ultrasonic power. It was also observed that the piezo-photocatalytic activity increased by increasing the ultrasonic irradiation. In the same investigation, authors reported that the dye does not degrade in the presence of ultrasonic power without UV irradiation, which is contrary to the literature reporting on Ag_2O/T-ZnO nanostructures generating piezoelectric field under ultrasonic vibrations alone.   On the other hand, the reported ultrafast dye degradation was mainly attributed to the absorption changes during catalysis and more evidence for the observed ultrafast dye degradation are needed to confirm such a rapid dye degradation.

As shown in Figure 8, the p-n junction is formed between p-type Ag_2O and n-type ZnO leading to the built-in electric field in the Ag_2O-ZnO heterostructure. The direction of the built-in electric field in the depletion layer is from ZnO to Ag_2O while the strain on c-axis of ZnO nanostructures generates piezoelectric charges at the surface facilitating the rapid separation of the photogenerated charge lowering down the recombination rate. The degradation mechanism of organic molecules by piezophotocatalysis is similar to that of piezocatalysis in which the electrons and holes that are generated by the combined piezoelectric and photoexcitation effects react with oxygen molecules to generate •OH radicals via superoxide radical anions and the holes react with hydroxyl groups forming •OH

radicals. These radicals react with organic dyes and oxidize them into CO_2 and H_2O. With the working mechanism of coupling of the built-in electric field of heterostructures and the piezoelectric field of ZnO, a higher piezo-photocatalytic effect was observed for the degradation of organic dye solutions with ZnO nanowires [125] and Ag-coated ZnO nanowires [126] by Chang et al., and Xue et al., respectively. As ultrafast degradation rates of organic pollutions have been achieved with the piezo-photocatalytic activity of Ag_2O/ZnO nanostructures under ultrasonic/UV exposure, authors suggested that it has potential applications in industry. However, as the reported high degradation rates are only for low-levels of pollutant, further experiments have to be carried out to access the piezo-photocatalytic activity of Ag_2O/ZnO nanostructures at higher pollutant levels.
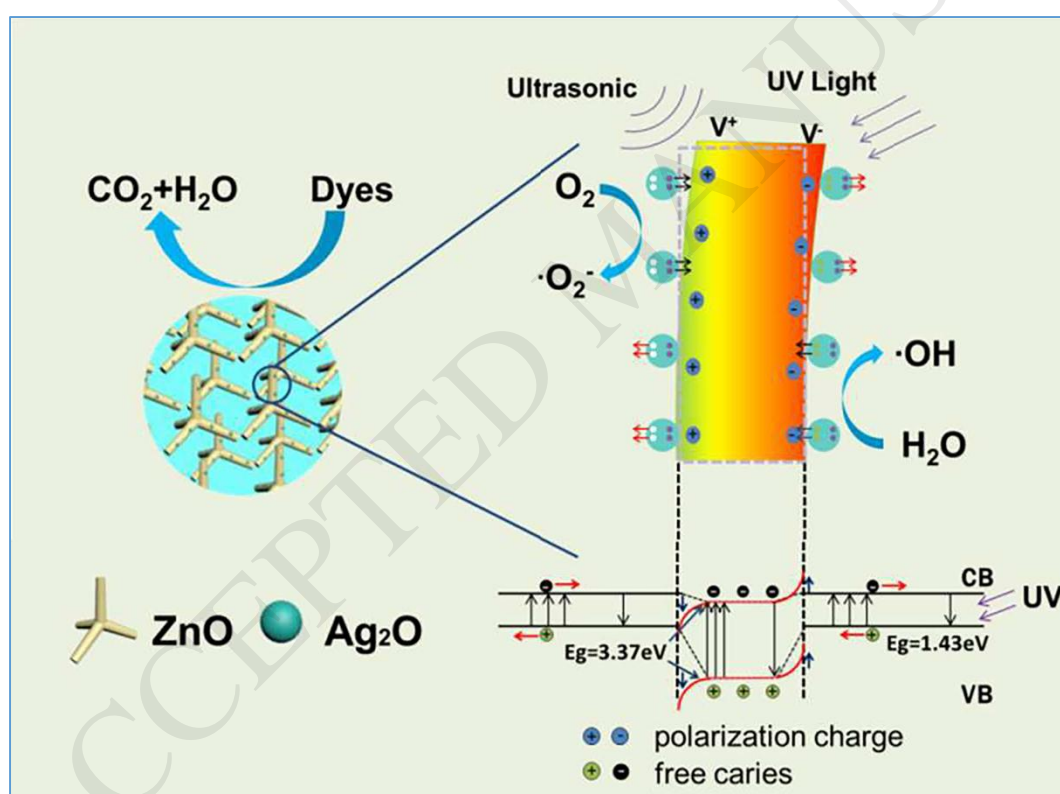
Figure 8. Schematic illustration showing the working mechanism for the piezo-photocatalytic process of Ag_2O/T-ZnO nanostructures under ultrasonic and UV exposure. Reproduced with permission [120].

Hong et al., continued their study to improve the piezophotocatalytic activity by coupling piezoelectric ZnO with the visible light active CuS photocatalyst to overcome the limited light absorption of piezoelectric ZnO [127]. By combining the piezoelectric ZnO nanowires and

visible light harvesting CuS, a CuS/ZnO heterostructure is formed and MB was removed within 20 min while in the same time frame, the concentration of MB is decreased to 37% by photocatalytic activity alone (Figure 9a). The enhanced catalytic activity of the CuS/ZnO heterostructured nanowire arrays on mesh was attributed to: (i) efficient light harvesting due to the large surface area, and (ii) to the coupling between the built-in electric field of the heterostructure and the piezoelectric field of ZnO under strain. As shown in Figure 9b, a built-in electric field created at the CuS/ZnO interface directs the photogenerated electrons in the CB of CuS into the CB of ZnO while the photogenerated holes transfer in the opposite direction from the VB of ZnO to that of CuS. Additionally, the piezoelectric field created by ZnO nanowires can further separate the photogenerated electrons/holes and lower down the recombination rate leading to enhanced photocatalytic activity. In their experiment, Hong et al demonstrated that under only ultrasound, the degradation of MB by bare ZnO nanowires and CuS/ZnO nanowires is very limited. MB could not be degraded under the mechanical vibration of ZnO nanowires (piezoelectric catalysis). However, the degradation results presented by Xu et al., and Li at al., by using ZnO nanorods and ZnO nanorods/MWCNT clearly showed the piezocatalytic degradation of AO7 and MB [85, 90-91]. Hence, a further piezocatalytic investigation has to be carried out with ZnO and coupled ZnO nanostructures (i.e CuS/ZnO) to define the role of ZnO in the coupled piezocatalytic system. The visible response of the   hetero-structured piezophotocatalyst was further enhanced by coupling of ZnO with Ag_2S (Ag_2S/ZnO) [128], Ag nanoparticles [129] and Au nanoparticles (Au/ZnO) [130]. When ZnO nanotetrapods were coupled with noble metal nanocrystals (Ag) where the localized surface plasmon resonance (LSPR) of Ag broaden the spectral response to visible range and the ohmic contact at the Ag/ZnO interface could probably facilitate the interfacial charge transfer [129, 131]. The piezoelectric field originated from the deformation of ZnO nanotetrapods enhances the separation of photo-induced electron/hole pairs leading to complete removal of MO within 25 min under ultrasonic stimulation (200 W) and solar illumination (500 W) [129].
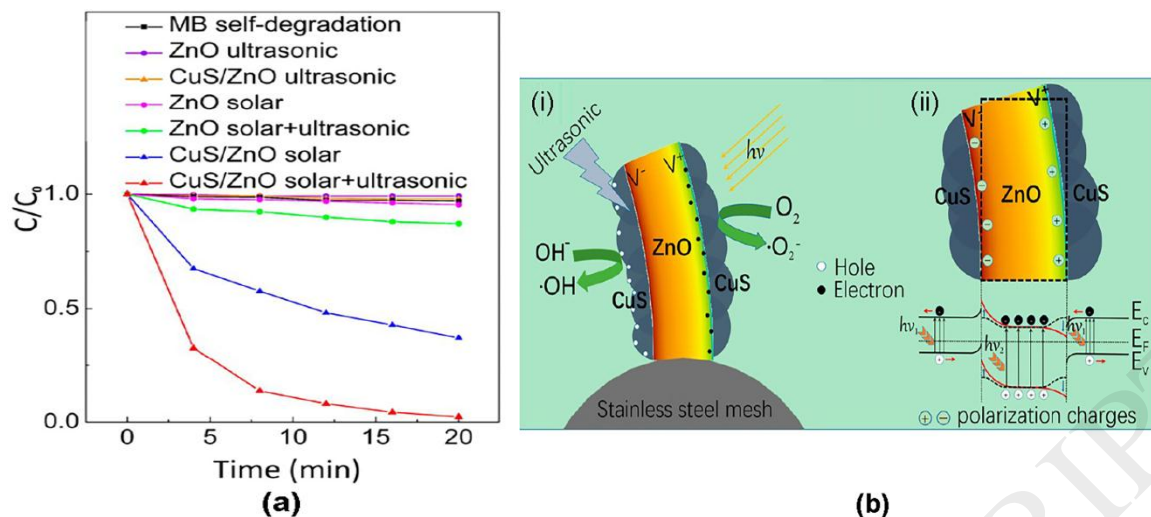
Figure 9. (a) Piezo-photocatalytic degradation profiles of MB as a function of irradiation time for bare ZnO and CuS/ZnO nanowires on the mesh under different conditions, (b,i) Schematic illustration showing the piezo-photocatalytic process of CuS/ZnO nanowires on stainless steel mesh under both solar and ultrasonic irradiation. (b, ii) Schematic illustration showing the energy band diagram of CuS/ZnO heterostructure under both solar and ultrasonic irradiation. Reproduced with permission [127].

You et al. [132] investigated a piezoelectric-photocatalytic system that consists of a heterostructure piezoelectric-ZnO@photoelectric-TiO$_2$ core-shell interface for the degradation of MO. The proposed piezoelectric-photocatalytic mechanism was similar to that of CuS/ZnO [127]. Though the coupled piezoelectric@photoelectric core-shell catalytic systems have been developed successfully, the individual contribution of the piezoelectric as well as the photoelectric materials in the piezoelectric@photoelectric core-shell catalytic systems is not yet clearly demonstrated. The understanding of the functions of piezoelectric and photoelectric materials in the coupled systems is vital for further enhancement of the bi-catalytic activity of piezoelectric@photoelectric core-shell catalytic systems. In a similar manner to applying mechanical stress on piezoelectric materials, Wang et al., modulated the strain in a piezoelectric ZnO by thermal sintering. Through cooling the hybrid TiO$_2$ nanoparticles on ZnO monocrystalline platelets heterojunction from high temperature to room temperature, due to the difference in the thermal expansion coefficients of the two materials it was able to introduce a piezopotential to the TiO$_2$/ZnO nanostructure. The piezopotential induced by the thermal sintering in the TiO$_2$/ZnO nanostructure enhanced the piezophotocatalytic degradations of MO and MB on the ZnO/TiO$_2$ hybrid catalyst [133]. However, it is not clear whether the strain introduced by in a piezoelectric ZnO by thermal

24

sintering is permanent or not as authors have not demonstrated the long-term piezophotocatatlytic activity. On the other hand, the strain introduction to piezoelectric materials by thermal expansion is much more complicated compared to the simple ultrasonic or stirring methods. In another report, high-frequency ultrasound as a selective advanced oxidation process to remove penicillin antibiotics from water has been recently reported by Sema-Galvis et al., [134]. The same research group reported on the mechanism and range of treatment for the degradation of a β-lactam antibiotic by TiO_2 photocatalysis compared to sonochemistry, electrochemistry and the photo-Fenton systems [135].

In 2012, Dai et al. [136] reported the use of an organic piezoelectric material, PVDF-(Polyvinylidene fluoride, which is an emerging piezoelectric polymer) [137, 138] for the preparation of the piezoelectric-photocatalytic heterostructure showing charge generation and separation as well as a solution to recover the used catalyst. TiO_2 nanoparticles [136] and fibers [139] were embedded in piezoelectric PVDF and resultant films showed easy recovery of the catalyst after the reaction. In addition, as the PVDF film being flexible, it is capable of sustaining larger strains compared to the inorganic counterparts. Dong et al., used hybrid PVDF/TiO_2 nanofibers and a flexible self-powering/self-cleaning electronic-skin (e-skin) was fabricated for the degradation of organic pollutants. The PVDF/TiO_2 nanofiber e-skin degrades organic pollutants under external mechanical vibration (in this case body movement) and UV irradiation [139]. The MB dye was completely degraded within 40 min using the e-skin under both ultrasonic (or low-frequency mechanical vibration) and UV irradiation which is similar to the self-cleaning behavior of the e-skin. As shown in Figure 10a and b, e-skin responses to different body motions (such as pressing, stretching, bending finger and clenching) due to the piezoelectric effect of PVDF and as a result, it has a self-cleaning characteristic through piezo-photocatalytic coupling process.

He et al., used the piezoelectric PVDF and tetrapod ZnO (T-ZnO) nanostructures to design an e-skin on the flexible fabric substrate and was able to degrade/sterilize organic-pollutants/bacteria at the e-skin interface [140]. The piezoelectric effect of both ZnO nanostructure and PVDF polymer convert mechanical vibration, i.e. in this case body motion, to generate $^\bullet OH$ and $O_2^{\bullet-}$ leading to the self-cleaning characteristics (Figure 10c and d). The

25

piezoelectric effect of ZnO nanostructure enhances the photo-excited charge carriers separation in ZnO probably lead to the enhanced self-cleaning behavior of the e-skin. After 10 min under UV/ultrasonic irradiation of a piece of e-skin containing 200 mg T-ZnO nanostructures and 100 mL organic dye aqueous solution (5 mg/L), the degradation percentages of MB, methyl orange, rhodamine B, congo red and phenol red are ~100%, ~90%, ~98%, ~100%, ~94% and ~92% respectively. In both PVDF/TiO$_2$ nanofibers and PVDF/ZnO based self-cleaning systems, the photogenerated electrons/holes under UV irradiation (~ 300 nm) participate in the degradation of organic pollutants. As UV radiations are harmful to skin, it would be safer if visible light active piezophotocatalysts can be used to design an e-skin. However, it should be mentioned that the majority of highly visible light active photocatalysts are non-piezoelectric and it will be a daunting challenge to synthesize highly visible light active piezoelectric material.
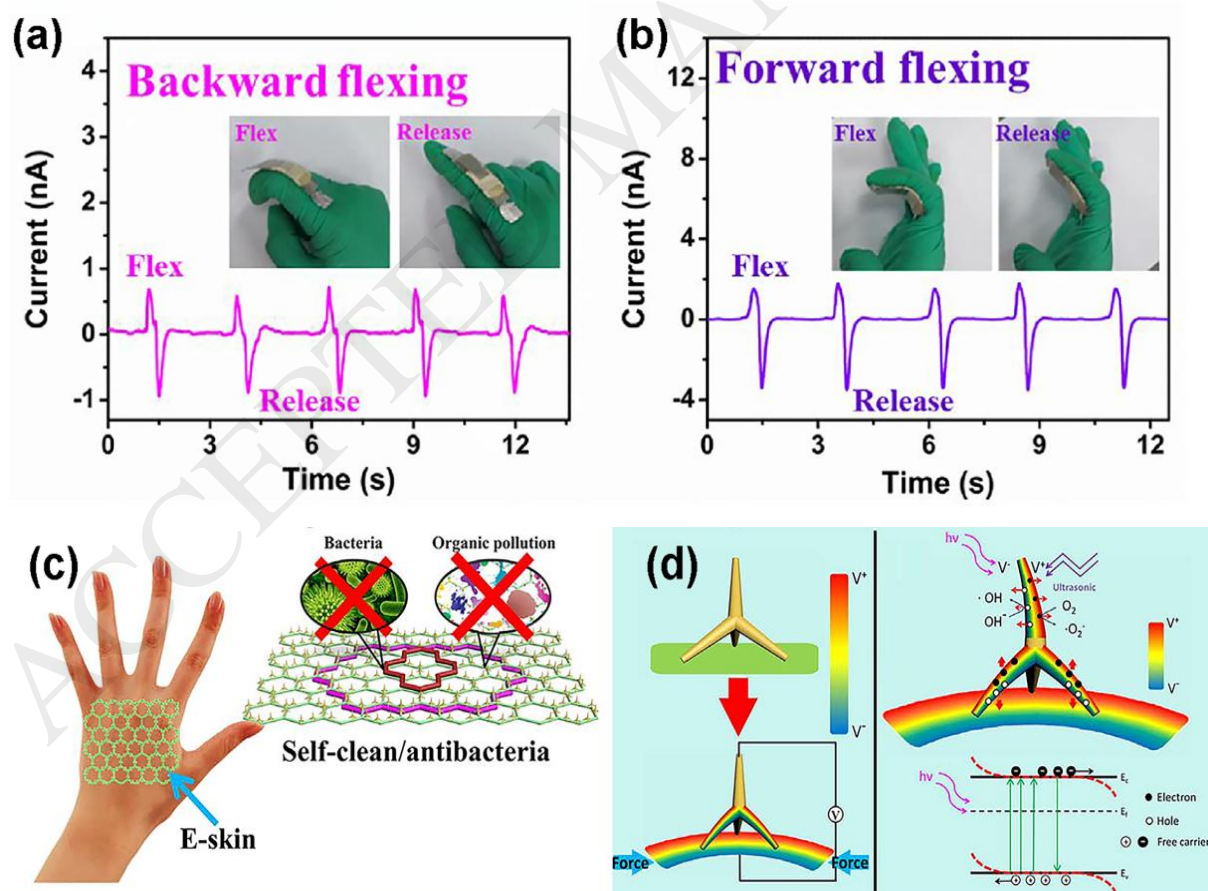

Figure 10. The flexible self-powering e-skin can actively detect body motion. The outputting piezoelectric current of the e-skin placing on the finger with (a) backward and (b) forward backward bending movement

26

respectively. Reproduced with permission [139]. (c) The T-ZnO/PVDF/fabric e-skin and (d) the piezoelectric/photocatalytic coupling effect for self-clean behaviors of the T-ZnO/PVDF/fabric e-skin. Reproduced with permission [140].

The single piezoelectric material that possesses photocatalytic properties are rare and finding new piezophotocatalysts is challenging. Huang et al., illustrated the use of non-centrosymmetric piezoelectric and photoactive $BiOIO_3$ semiconductor for the photo- and piezoelectric-induced molecular oxygen activation and RhB dye degradation [141]. The layered bismuth-based materials, such as sillen-structured BiOX (X=Br, I, Cl), [142] aurivillius structured Bi_2XO_6 (X=Mo, W) [143] and sillen-structure-related $(BiO)_2CO_3$ [144], are classes of photocatalyst that contain layered bismuth-based materials that support the formation of an internal electric field due to their non-centrosymmetric nature. The macroscopic polarization of $BiOIO_3$ was enhanced by the replacement of V^{5+} ions for I^{5+} in IO_3 polyhedra. As a result, 1.7 and 3.3 times higher piezoelectric-catalytic $O_2^-\cdot$ and $\cdot OH$ evolution rates were reported for $BiOI_{0.926}V_{0.074}O_3$ compared to pure $BiOIO_3$ [141]. Although the large macroscopic polarization of $BiOI_{0.0926}V_{0.074}O_3$ and $BiOIO_3$ was demonstrated by SHG signal, authors have not demonstrated the vital piezoelectric properties such as the piezoelectric coefficients of both of $BiOI_{0.0926}V_{0.074}O_3$ and $BiOIO_3$. On the other hand, the role of V^{5+} in enhancing the polarization in $BiOIO_3$ has been analyzed by polyhedral distortion index where a higher polyhedral distortion in $BiOI_{0.0926}V_{0.074}O_3$ was observed and hence a higher macroscopic polarization in $BiOI_{0.0926}V_{0.074}O_3$. However, further understanding of the effect/role of I^{5+} replacement in $BiOIO_3$ by different cations is important to realize the single piezoelectric material that possesses photocatalytic properties as well.

To enhance the charge separation further in narrow band gap BiOI photocatalytic semiconductor nanoparticles, Huang et al., used ferroelectric tetragonal-phase $T-BaTiO_3$ and nonferroelectric cubic-phase $C-BaTiO_3$ to construct photocatalytic-piezoelectric heterostructures with BiOI [145]. The MO dye degradation rate (95.4% of MO is decomposed over 90 min periods) and reactive superoxide radical $O_2^-\cdot$ production rates (11.02×10^{-7} $mol\cdot L^{-1}\cdot h^{-1}$) are higher in ferroelectric $T-BaTiO_3$/BiOI than that of $C-BaTiO_3$/BiOI which is attributed to the enhanced charge separation of BiOI under the influence of piezoelectric $T-BaTiO_3$. Sillen-structure $Bi_2O_2(OH)(NO_3)$ nanosheet was tested for piezophotocatalytic

27

degradation of organic dyes and antibiotic by Hao et al., [146]. A facet dependent efficient charge separation was noted where the dominant exposure of <0 0 1> reactive facet in the $Bi_2O_2(OH)(NO_3)$ nanosheet leading to efficient charge separation than that of bulk $Bi_2O_2(OH)(NO_3)$. The $\cdot OH$ evolution rates of nanosheet and bulk $Bi_2O_2(OH)(NO_3)$ were 7.13 and 0.029 $\mu mol \cdot L^{-1} \cdot h^{-1}$ respectively. Similarly, $Bi_2O_2(OH)(NO_3)$ nanosheets degraded 30.3% and 56.4% of BPA and tetracycline hydrochloride after 5 h of ultrasonic treatment respectively.

Dai et al., further developed the piezoelectric-based photocatalyst by coupling TiO_2 with a high piezoelectric material i.e. lead magnesium niobate-leadtitanate $0.675Pb(Mg_{1/3}Nb_{2/3})O_3$ -$0.325PbTiO_3$(PMN-PT) [147] that possesses a high piezoelectric coefficient d_{33} of 2500 pm/V. Promising new generation of piezoelectric materials, which have much higher piezoelectric coefficient than that of $BaTiO_3$ ($d_{33} = 80$ pm/V) and ZnO (27 pm/V) were investigated by Kumar et al., Xu et al.,[148, 149]. By coupling PMN-PT with TiO_2, piezocatalytic activity of TiO_2 is increased significantly. In the presence of PMN-PT and PMN-PT@TiO_2 under sonication resulted in 15 and 18% degradation of RhB, while under the same conditions and in the presence of light resulted in 75 and 85% degradation rates respectively. The same authors embedded the PMN-PT@TiO_2 piezocatalyst in the Poly-dimethylsiloxane (PDMS) matrix for the enhancement of the stability over several runs [150]. It is known that $ZnSnO_3$ is a piezoelectric material that possesses a high piezoelectric coefficient [151, 152]. Lo et al., investigated the piezophotocatalytic nature of the novel $ZnSnO_3$-nanowire for achieving a synergistic catalytic performance as its piezoelectric coefficient (~ 59 $\mu C/cm^2$) is higher than that of ZnO (~ 5 $\mu C/cm^2$) [153]. In their piezocatalytic experiment, by modulating the piezopotential across the $ZnSnO_3$, enhanced photocatalytic degradation ($\sim$ by 27%) of MB was reported and the higher catalytic activity was attributed to its high piezoelectric coefficient. The same authors tested the Zn-deficient $ZnSnO_3$ nanowire for piezophototronic effect where a higher piezoelectric was reported for the Zn-deficient $Zn_{1-x}SnO_3$ nanowire than that of $ZnSnO_3$. Consequently, a higher piezophotocatalytic activity was reported with $Zn_{1-x}SnO_3$ nanowire in the degradation of MB [154]. Though a definite reason was not given for the observed higher piezoelectric properties

of Zn deficient $Zn_{1-x}SnO_3$ nanowire, as described earlier it could be due to the presence of free charge carriers and defects in $Zn_{1-x}SnO_3$ nanowire.   Lin et al., further enhanced the piezocatalytic activity of $ZnSnO_3$ by fixing them in functional polymer poly(vinylidene fluoride) (PVDF) – or poly (methyl methacrylate) (PMMA) [155]. A reaction rate constant of 11.4×10^{-3} min^{-1} is reported for the piezophotocatalytic degradation of MB. The degradation rate was three times higher than that of the pure ZTO sample. The higher piezophotocataltyic activity was attributed to the effective contact between nanocomposites and stress sources through flexible PVDF or PMMA matrix leading to a better transfer of mechanical energy. Though it is not likely to compare the piezocatalytic activities of high piezoelectric material (i.e . lead magnesium niobate-leadtitanate, piezoelectric coefficient 2500 pm/V) [147] and low piezoelectric material ($BaTiO_3$, piezoelectric coefficient 80 pm/V) [64, 84] as their surface areas were not clearly reported. Nonetheless, when the dye degradations were carried out under similar conditions with both $PbTiO_3$ and $BaTiO_3$ indicated that the piezocatalytic activity is less dependent on the piezoelectric coefficient. Similar results has been observed with $Zn_{1-x}SnO_3$ ($\sim$ 59 $\mu C/cm^2$) [154, 155] and ZnO ($\sim$ 5 $\mu C/cm^2$) [125]. Therefore, more experiments are needed to verify the role of piezoelectric strength on the piezocatalytic activity.

In order to overcome the stability problem of the common piezoelectric materials such as ZnO and $BaTiO_3$, Singh et al. used a chemically stable $NaNbO_3$ piezoelectric semiconductor as a novel piezoelectric material as well as a semiconductor photocatalyst [156]. As demonstrated by Singh et al. chemically stable $NaNbO_3$ is a good single phase compound to demonstrate the efficient coupling between piezoelectric, semiconducting and photoexcitation properties. The built-in-potential generated in $NaNbO_3$ under mechanical strain improves the photogenerated charge carrier separation and $NaNbO_3$ particulate suspension shows enhancement in the photodegradation rate of organic dyes by ~115%, which is much higher than the earlier reported piezophotocatalytic activity in ZnO. The high piezophotocatalytic activity was attributed to the high piezoelectric potential and high mobility of charge carriers in $NaNbO_3$.

Piezoelectric materials such as lead zirconate titanate and polyvinylidene fluoride (PVDF)

were also successfully employed to remove the fouling, i.e. the accumulation of unwanted macromolecules materials such as proteins and particle deposits on filtering membranes used in waste treatments resulting in declining in the permeate flux during filtration [157-163]. These accumulated materials are difficult to remove even with severe chemical treatments and fouling removal by the piezoelectric effect is presumably due to their local turbulence [157]. The piezoelectric properties of piezoelectric membranes were activated by polarizing the materials in the membrane in the same direction by applying a high voltage. The membranes were fabricated by conventional methods but incorporating piezoelectric materials. Since the use of piezoelectric membranes for removal of fouling materials is rather a physical process than a catalytic process, detailed discussions are beyond the scope of the present review.

2.4 Application of Piezophotocatalytic materials in water splitting

Another application of piezoelectric materials is the piezocatalytic production of H_2 by water splitting. Hong et al. used piezoelectric ZnO microfibres and $BaTiO_3$ micro-dendrites to produce H_2 by harvesting vibrations [76]. A stoichiometric ratio of H_2 and O_2 gas production was noted when ZnO fibers and $BaTiO_3$ micro dendrites were subjected to ultrasonic vibrations in pure water and the hydrogen production efficiency is depended on the fiber length and the aspect ratio. However, due to the limitation of the deflection in branch-like $BaTiO_3$ structures, a lower gas production rate was observed. The hydrogen production by the piezocatalytic process by scavenging energy waste is simple and cost-effective. The fundamental processes taking place at the surface of the piezoelectric materials during piezoelectric-potential driven electrochemical H_2 evolution reaction [164] are similar to that of piezocatalytic degradation of organic pollutants described in the section 2.2.1 [49, 53]. Here, the reactive species that develop on the piezoelectric materials by the mechanical stress contribute to water reduction-oxidation reactions on the positive and negative surfaces of the piezoelectric material. The developed free charges that are having a potential higher than 1.23 eV react with water and produces H_2. Tan et al., coupled visible light harvesting Ag/Ag_2S semiconductor nanoparticles with the piezoelectric ZnO nanorods to enhance the charge separation in $Ag/Ag_2S–ZnO/ZnS$ semiconductor-piezoelectric heterojunction. They used this composite in a photo-electrochemical (PEC) water splitting device [85] and photocurrent

30

densities of 22 and 8 mA.m^{-2} were observed with the vibration and without vibrations respectively.   The enhanced photocurrent density has been attributed to the applied sonication. The charges generated in Ag/Ag$_2$S–ZnO/ZnS photoanode were due to sonication and transfer from photoanode to Pt counter electrode creating a self-biasing in Ag/Ag$_2$S–ZnO/ZnS photoanode. In the water splitting process, photogenerated holes were released to the electrolyte solution leaving electrons in the anode. These photogenerated electrons then move toward the Pt counter electrode. Zhang et al., proposed a piezoelectrochemical hydrogen production device integrating a piezoelectric bimorph cantilever to a water electrolyzer [165]. The hydrogen production rate of 10^{-8} mol/min with a piezoelectric PZT-5 ceramic plate combined with a water electrolyzer is weak due to the poor conversion efficiency of the applied mechanical energy to electric energy (~ 36%). Though the hydrogen production via piezoelectric effect is cost-effective and environment-friendly, much progress in this direction has not been achieved.

3. Prospective and summary - Conclusions and outlook

In this review, the exploitation of the in-built potential of piezoelectric materials in catalytic and photocatalytic applications was illustrated comprehensively and the progress to-date on catalytic/photocatalytic activities based on piezoelectric effects was discussed. The review contains a discussion on the fundamentals of piezoelectric effects, such as the stress-induced polarization and the origin of such polarization followed by a discussion on the use of piezoelectric materials for piezocatalytic and piezophotocatalytic processes. The effect of the internal electric field in charge separation in piezoelectric materials under the mechanical stress and their use in piezocatalytic degradation of pollutants were discussed in the first section. In the second section, the effect of the induced internal electric field in charge carrier generation and separation in piezophotocatalysts and their use in the degradation of pollutants with piezophotocatalyts were discussed. Lastly, the work done on the use of piezoelectric materials for water splitting was briefly illustrated.

Recent studies showed that the piezocatalysis and piezophotocatalysis are a new approach that enables enhancing the electrochemical processes at the surface by the polarization of charges, which promote different carriers to move to spatially different locations. The induced

electric field within the piezoelectric material by exerting the mechanical stress augments the energetics of both free and bound charges throughout the material leading to enhanced redox catalytic reaction at the surface. Piezocatalysis as well as piezophotocatalysis were shown not be depended on pH. Likewise, pollutants degradation efficiency with the mass of the piezocatalyst does not significantly control the reaction rate but the observed variations are not significant and further research has to be carried out. The piezoelectric properties of the materials are more important than their morphological structure (1-D or 2-D). The presence of free charges in the piezoelectric materials is imperative to be piezocatalytically active. Piezoelectric materials having high piezoelectric coefficient and high carriers density are the most appropriate piezocatalysts. The intrinsic charge carrier density is the key factor in charge transfer in the piezocatalysis process. The piezoelectric charges in piezoelectric crystallites are shown to be less critical for the charge transfer. Henceforward, piezocatalytic process can be enhanced through regulating the concentration of charge carriers. On the other hand, the use of the flexible piezoelectric organic polymer in piezoelectric-catalyst heterostructure increases the strains on the embedded catalyst compared with inorganic counterparts enabling higher degradation rates of organic pollutants. This was attributed to the enhanced charge carrier generation and separation. On the other hand, a single piezoelectric material that possesses photocatalytic properties is rare. The preparation of new piezophotocatalysts is vital for applying these catalysts for environmental remediation. The piezoelectric charges at the surface of piezoelectric material-semiconductor junction (coupling of piezoelectric and semiconductor materials) facilitate rapid separation of the photogenerated electrons/holes, lowering down the recombination rate and enhancing the photocatalytic efficiency. Specifically, the formation of a p-n junction between n-type piezoelectric material and p-type semiconductor could realize the maximum charge separation. By coupling piezoelectric materials with the visible light active semiconductor photocatalysts or noble metal nanocrystals with a localized surface plasmon resonance can help to overcome the limited light absorption of piezoelectric materials.

Finally, the piezoelectric materials alone or coupled to another semiconductor is an alternative and a reliable method that can be used in environmental remediation. However, the

present knowledge on piezoelectric catalysis as well as piezophotocatalysis do not warranty an immediate application, but once developed, it would pave in the making of new and ideal catalytic and photocatalytic systems for environmental remediation.

Conflicts of interest

There are no conflicts to declare.

Acknowledgement

References

[1] S.H. Park, W.C. Labys, Industrial Development and Environmental Degradation, Books, (2015).

[2] Y.C. Ho, K.Y. Show, X.X. Guo, I. Norli, F.M.A. Abbas, N. Morad, Industrial Discharge and Their Effect to the Environment, InTech2012.

[3] P. Mudu, B. Terracini, M. Martuzzi, Human health in areas with industrial contamination, WHO Regional Office for Europe, Copenhagen, 2014.

[4] K. Remoundou, P. Koundouri, Environmental Effects on Public Health: An Economic Perspective, Int J Env Res Pub He, 6 (2009) 2160-2178.

[5] S. Rtimi, S. Giannakis, M. Bensimon, C. Pulgarin, R. Sanjines, J. Kiwi, Supported TiO2 films deposited at different energies: Implications of the surface compactness on the catalytic kinetics, Appl Catal B-Environ, 191 (2016) 42-52.

[6] J. Bandara, U. Klehm, J. Kiwi, Raschig rings-Fe2O3 composite photocatalyst activate in the degradation of 4-chlorophenol and Orange II under daylight irradiation, Appl Catal B-Environ, 76 (2007) 73-81.

[7] G. Mamba, C. Pulgarin, J. Kiwi, M. Bensimon, S. Rtimi, Synchronic coupling of Cu 2 O(p)/CuO(n) semiconductors leading to Norfloxacin degradation under visible light: Kinetics, mechanism and film surface properties, Journal of Catalysis, 353 (2017) 133-140.

[8] S. Rtimi, O. Baghriche, C. Pulgarin, R. Sanjines, J. Kiwi, Design, testing and characterization of innovative TiN-TiO2 surfaces inactivating bacteria under low intensity visible light, Rsc Adv, 2 (2012) 8591-8595.

[9] S. Rtimi, C. Pulgarin, R. Sanjines, J. Kiwi, Innovative semi-transparent nanocomposite films presenting photo-switchable behavior and leading to a reduction of the risk of infection under sunlight, Rsc Adv, 3 (2013) 16345.

[10] O. Baghriche, S. Rtimi, C. Pulgarin, J. Kiwi, Polystyrene CuO/Cu2O uniform films inducing MB-degradation under sunlight, Catalysis Today, 284 (2017) 77-83.

[11] K. Tennakone, J. Bandara, Multiphoton semiconductor photocatalysis, Solar Energy Materials & Solar Cells, 60 (2000) 361-365.

[12] J. Bandara, J. Kiwi, †, C. Pulgarin, P. Peringer, G.M. Pajonk, a. A. Elaloui, P. Albers⊥, Novel Cyclic Process Mediated by Copper Oxides Active in the Degradation of Nitrophenols: Implications for the Natural Cycle, Environ Sci Technol, 30 (1996) 1261-1267.

[13] A.H. Mamaghani, F. Haghighat, C.S. Lee, Photocatalytic oxidation technology for indoor environment air purification: The state-of-the-art, Appl Catal B-Environ, 203 (2017) 247-269.

[14] J.L. Wang, L.J. Xu, Advanced Oxidation Processes for Wastewater Treatment: Formation of Hydroxyl Radical and Application, Crit Rev Env Sci Tec, 42 (2012) 251-325.

[15] L.W. Zhang, H.H. Mohamed, R. Dillert, D. Bahnemann, Kinetics and mechanisms of charge transfer processes in photocatalytic systems: A review, J Photoch Photobio C, 13 (2012) 263-276.

[16] M.N. Chong, B. Jin, C.W.K. Chow, C. Saint, Recent developments in photocatalytic water treatment technology: A review, Water Res, 44 (2010) 2997-3027.

[17] S.Y. Dong, J.L. Feng, M.H. Fan, Y.Q. Pi, L.M. Hu, X. Han, M.L. Liu, J.Y. Sun, J.H. Sun, Recent developments in heterogeneous photocatalytic water treatment using visible light-responsive photocatalysts: a review, Rsc Adv, 5 (2015) 14610-14630.

[18] S. Bagheri, A. TermehYousefi, T.O. Do, Photocatalytic pathway toward degradation of environmental pharmaceutical pollutants: structure, kinetics and mechanism approach, Catal Sci Technol, 7 (2017) 4548-4569.

[19] Z.P. Wang, J.M. Song, F. Gao, R. Su, D.W. Zhang, Y. Liu, C.C. Xu, X.J. Lou, Y.D. Yang, Developing a ferroelectric nanohybrid for enhanced photocatalysis, Chem Commun, 53 (2017) 7596-7599.

[20] A. Kakekhani, S. Ismail-Beigi, Ferroelectric-Based Catalysis: Switchable Surface Chemistry, Acs Catal, 5

(2015) 4537-4545.

[21] A. Kakekhani, S. Ismail-Beigi, E.I. Altman, Ferroelectrics: A pathway to switchable surface chemistry and catalysis, Surf Sci, 650 (2016) 302-316.

[22] J. Zhang, C.Y. Wang, C. Bowen, Piezoelectric effects and electromechanical theories at the nanoscale, Nanoscale, 6 (2014) 13314-13327.

[23] J.M. Wu, Y.G. Sun, W.E. Chang, J.T. Lee, Piezoelectricity induced water splitting and formation of hydroxyl radical from active edge sites of MoS2 nanoflowers, Nano Energy, 46 (2018) 372-382.

[24] Y.F. Hu, C.F. Pan, Z.L. Wang, Recent progress in piezo-phototronics with extended materials, application areas and understanding, Semicond Sci Tech, 32 (2017).

[25] H.X. Li, Y.H. Yu, M.B. Starr, Z.D. Li, X.D. Wang, Piezotronic-Enhanced Photoelectrochemical Reactions in Ni(OH)(2)-Decorated ZnO Photoanodes, J Phys Chem Lett, 6 (2015) 3410-3416.

[26] C.R. Bowen, H.A. Kim, P.M. Weaver, S. Dunn, Piezoelectric and ferroelectric materials and structures for energy harvesting applications, Energ Environ Sci, 7 (2014) 25-44.

[27] D. Damjanovic, Ferroelectric, dielectric and piezoelectric properties of ferroelectric thin films and ceramics, Rep Prog Phys, 61 (1998) 1267-1324.

[28] D. Damjanovic, Chapter 4 - Hysteresis in Piezoelectric and Ferroelectric Materials A2 - Bertotti, Giorgio, in: I.D. Mayergoyz (Ed.) The Science of Hysteresis, Academic Press, Oxford, 2006, pp. 337-465.

[29] J. Curie, P. Curie, Development, via compression, of electric polarization in hemihedral crystals with inclined faces, Bulletin de la Societe de Minerologique de France, 3 (1880) 90-93.

[30] R.S. Dahiya, M. Valle, Tactile Sensing Technologies, Robotic Tactile Sensing: Technologies and System, Springer Netherlands, Dordrecht, 2013, pp. 79-136.

[31] G. Mantini, Y.F. Gao, A. D'Amico, C. Falconi, Z.L. Wang, Equilibrium Piezoelectric Potential Distribution in a Deformed ZnO Nanowire, Nano Res, 2 (2009) 624-629.

[32] Z. Gao, J. Zhou, Y. Gu, P. Fei, Y. Hao, G. Bao, Z.L. Wang, Effects of piezoelectric potential on the transport characteristics of metal-ZnO nanowire-metal field effect transistor, J Appl Phys, 105 (2009) 113707.

[33] Z.L. Wang, J.H. Song, Piezoelectric nanogenerators based on zinc oxide nanowire arrays, Science, 312 (2006) 242-246.

[34] Z.L. Wang, Piezopotential gated nanowire devices: Piezotronics and piezo-phototronics, Nano Today, 5 (2010) 540-552.

[35] K.C. Kao, 4 – Ferroelectrics, Piezoelectrics, and Pyroelectrics, Dielectric Phenomena in Solids, (2004) 213-282.

[36] C.H. Ahn, K.M. Rabe, J.M. Triscone, Ferroelectricity at the nanoscale: Local polarization in oxide thin films and heterostructures, Science, 303 (2004) 488-491.

[37] P.P. Shi, Y.Y. Tang, P.F. Li, W.Q. Liao, Z.X. Wang, Q. Ye, R.G. Xiong, Symmetry breaking in molecular ferroelectrics, Chem Soc Rev, 45 (2016) 3811-3827.

[38] A.L. Kholkin, N.A. Pertsev, A.V. Goltsev, Piezoelectricity and Crystal Symmetry, in: A. Safari, E.K. Akdoğan (Eds.) Piezoelectric and Acoustic Materials for Transducer Applications, Springer US, Boston, MA, 2008, pp. 17-38.

[39] Y.-R. Wu, J. Singh, Transient study of self-heating effects in AlGaN/GaN HFETs: Consequence of carrier velocities, temperature, and device performance, Journal of applied physics, 101 (2007) 113712.

[40] C.R. Bowen, J. Taylor, E. LeBoulbar, D. Zabek, A. Chauhan, R. Vaish, Pyroelectric materials and devices for energy harvesting applications, Energy & Environmental Science, 7 (2014) 3836-3856.

[41] J. Varghese, R.W. Whatmore, J.D. Holmes, Ferroelectric nanoparticles, wires and tubes: synthesis, characterisation and applications, J Mater Chem C, 1 (2013) 2618-2638.

[42] R. Manabe, S. Okada, R. Inagaki, K. Oshima, S. Ogo, Y. Sekine, Surface Protonics Promotes Catalysis, Sci Rep-Uk, 6 (2016) 38007.

[43] Z.L. Wang, W.Z. Wu, Piezotronics and piezo-phototronics: fundamentals and applications, Natl Sci Rev, 1 (2014) 62-90.

[44] J. Shi, M.B. Starr, X.D. Wang, Band Structure Engineering at Heterojunction Interfaces via the Piezotronic Effect, Adv Mater, 24 (2012) 4683-4691.

[45] S. Anand, K. Thekkepat, U.V. Waghmare, Two-Dimensional Rectangular and Honeycomb Lattices of NbN: Emergence of Piezoelectric and Photocatalytic Properties at Nanoscale, Nano Lett, 16 (2016) 126-131.

[46] R. Tao, M. Mouis, G. Ardila, Unveiling the Influence of Surface Fermi Level Pinning on the Piezoelectric Response of Semiconducting Nanowires, Adv Electron Mater, 4 (2018) 1700299.

[47] Z.L. Wang, Progress in Piezotronics and Piezo-Phototronics, Adv Mater, 24 (2012) 4632-4646.

[48] P.M. Jones, S. Dunn, Interaction of Stern layer and domain structure on photochemistry of lead-zirconate-titanate, Journal of Physics D: Applied Physics, 42 (2009) 065408.

[49] M.B. Starr, X.D. Wang, Coupling of piezoelectric effect with electrochemical processes, Nano Energy, 14 (2015) 296-311.

[50] L. Li, P.A. Salvador, G.S. Rohrer, Photocatalysts with internal electric fields, Nanoscale, 6 (2014) 24-42.

[51] Y.F. Cui, J. Briscoe, S. Dunn, Effect of Ferroelectricity on Solar-Light-Driven Photocatalytic Activity of BaTiO3-Influence on the Carrier Separation and Stern Layer Formation, Chem Mater, 25 (2013) 4215-4223.

[52] X. Yang, D. Wang, Chapter Two - Photophysics and Photochemistry at the Semiconductor/Electrolyte Interface for Solar Water Splitting, in: Z. Mi, L. Wang, C. Jagadish (Eds.) Semiconductors and Semimetals, Elsevier2017, pp. 47-80.

[53] M.B. Starr, X. Wang, Fundamental Analysis of Piezocatalysis Process on the Surfaces of Strained Piezoelectric Materials, Sci Rep-Uk, 3 (2013) 2160.

[54] H. Li, C. Tian, Z.D. Deng, Energy harvesting from low frequency applications using piezoelectric materials, Applied Physics Reviews, 1 (2014) 041301.

[55] J. Briscoe, S. Dunn, Piezoelectric nanogenerators – a review of nanostructured piezoelectric energy harvesters, Nano Energy, 14 (2015) 15-29.

[56] W. Wu, Z.L. Wang, Piezotronics and piezo-phototronics for adaptive electronics and optoelectronics, Nature Reviews Materials, 24 (2016) 23-24.

[57] J.G. Webster, Encyclopedia of Medical Devices and Instrumentation, John Wiley & Sons, Inc.1989.

[58] K. Yang, D. Alice, Z. Meiling, A sandwiched piezoelectric transducer with flex end-caps for energy harvesting in large force environments, Journal of Physics D: Applied Physics, 50 (2017) 345501.

[59] C. Keplinger, J.Y. Sun, C.C. Foo, P. Rothemund, G.M. Whitesides, Z. Suo, Stretchable, transparent, ionic conductors, Science, 341 (2013) 984-987.

[60] Y.K. Fuh, C.C. Kuo, Z.M. Huang, S.C. Li, E.R. Liu, A Transparent and Flexible Graphene-Piezoelectric Fiber Generator, Small, 12 (2016) 1875-1881.

[61] X.H. Zhang, H.W. Ma, Study on Piezoelectric Effect and Magnetic Properties of Tourmalines, Advanced Materials Research, 1015 (2014) 259-263.

[62] G.W. Fox, G.A. Fink, The piezoelectric properties of quartz and tourmaline, Physics-J Gen Appl P, 5 (1934) 302-306.

[63] D. Vatansever, E. Siores, T. Shah, Alternative Resources for Renewable Energy: Piezoelectric and Photovoltaic Smart Structures, InTech2012.

[64] A. Khalal, D. Khatib, B. Jannot, Elastic and piezoelectric properties of BaTiO3 at room temperature, Physica B, 271 (1999) 343-347.

[65] A. Yourdkhani, G. Caruntu, Characterization of the Microstructural and Piezoelectric Properties of PbTiO3 Thin Films Synthesized by Liquid-Phase Deposition, J Phys Chem C, 115 (2011) 14797-14805.

[66] G. Shirane, S. Hoshino, K. Suzuki, X-Ray Study of the Phase Transition in Lead Titanate, Phys Rev, 80 (1950) 1105-1106.

[67] E. Sawaguchi, Ferroelectricity Versus Antiferroelectricity in the Solid Solutions of Pbzro3 and Pbtio3, J Phys Soc Jpn, 8 (1953) 615-629.

[68] B. Jaffe, R.S. Roth, S. Marzullo, Piezoelectric Properties of Lead Zirconate-Lead Titanate Solid-Solution Ceramics, J Appl Phys, 25 (1954) 809-810.

[69] M.A. Khan, M.A. Nadeem, H. Idrissn, Ferroelectric polarization effect on surface chemistry and photo-catalytic activity: A review, Surf Sci Rep, 71 (2016) 1-31.

[70] L.F. Wan, T. Nishimatsu, S.P. Beckman, The structural, dielectric, elastic, and piezoelectric properties of KNbO3 from first-principles methods, J Appl Phys, 111 (2012) 104107.

[71] V. Edon, D. Remiens, S. Saada, Structural, electrical and piezoelectric properties of LiNbO3 thin films for surface acoustic wave resonators applications, Appl Surf Sci, 256 (2009) 1455-1460.

[72] R.S. Weis, T.K. Gaylord, Lithium-Niobate - Summary of Physical-Properties and Crystal-Structure, Appl Phys a-Mater, 37 (1985) 191-203.

[73] R.T. Smith, F.S. Welsh, Temperature Dependence of Elastic, Piezoelectric, and Dielectric Constants of Lithium Tantalate and Lithium Niobate, J Appl Phys, 42 (1971) 2219-&.

[74] K. Heiji, The Piezoelectricity of Poly (vinylidene Fluoride), Japanese Journal of Applied Physics, 8 (1969) 975.

[75] J.C. Villar, S.L. Hidalgo, A.C. Penela, B.G. Meijide, A New Perspective for Labeling the Carbon Footprint Against Climate Change, in: B.R. Singh (Ed.) Global Warming - Impacts and Future Perspective, InTech, Rijeka, 2012, pp. Ch. 01.

[76] K.S. Hong, H.F. Xu, H. Konishi, X.C. Li, Direct Water Splitting Through Vibrating Piezoelectric Microfibers in Water, J Phys Chem Lett, 1 (2010) 997-1002.

[77] T.W. Hamann, F. Gstrein, B.S. Brunschwig, N.S. Lewis, Measurement of the free-energy dependence of interfacial charge-transfer rate constants using ZnO/H2O semiconductor/liquid contacts, J Am Chem Soc, 127 (2005) 7815-7824.

[78] T.W. Hamann, F. Gstrein, B.S. Brunschwig, N.S. Lewis, Measurement of the dependence of interfacial charge-transfer rate constants on the reorganization energy of redox species at n-ZnO/H2O interfaces, J Am Chem Soc, 127 (2005) 13949-13954.

[79] T.W. Hamann, F. Gstrein, B.S. Brunschwig, N.S. Lewis, Measurement of the driving force dependence of interfacial charge-transfer rate constants in response to pH changes at n-ZnO/H2O interfaces, Chem Phys, 326 (2006) 15-23.

[80] L.N. German, M.B. Starr, X. Wang, Computation of Electronic Energy Band Diagrams for Piezotronic Semiconductor and Electrochemical Systems, Adv Electron Mater, 4 (2018) 1700395.

[81] J. Wu, N. Qin, D.H. Bao, Effective enhancement of piezocatalytic activity of BaTiO3 nanowires under ultrasonic vibration, Nano Energy, 45 (2018) 44-51.

[82] X.P. Lin, J.C. Xing, W.D. Wang, Z.C. Shan, F.F. Xu, F.Q. Huang, Photocatalytic activities of heterojunction semiconductors Bi2O3/BaTiO3: A strategy for the design of efficient combined photocatalysts, J Phys Chem C, 111 (2007) 18288-18293.

[83] P. Wardman, Reduction Potentials of One-Electron Couples Involving Free-Radicals in Aqueous-Solution, J Phys Chem Ref Data, 18 (1989) 1637-1755.

[84] M. Acosta, N. Novak, V. Rojas, S. Patel, R. Vaish, J. Koruza, G.A. RossettiJr., J. Rödel, BaTiO3-based

piezoelectrics: Fundamentals, current status, and perspectives, Applied Physics Reviews, 4 (2017) 041305.

[85] C.F. Tan, W.L. Ong, G.W. Ho, Self-Biased Hybrid Piezoelectric-Photoelectrochemical Cell with Photocatalytic Functionalities, Acs Nano, 9 (2015) 7661-7670.

[86] S.C. Rai, K. Wang, J. Chen, J.K. Marmon, M. Bhatt, S. Wozny, Y. Zhang, W. Zhou, Enhanced Broad Band Photodetection through Piezo-Phototronic Effect in CdSe/ZnTe Core/Shell Nanowire Array, Adv Electron Mater, 1 (2015) 1400050.

[87] K.S. Hong, H.F. Xu, H. Konishi, X.C. Li, Piezoelectrochemical Effect: A New Mechanism for Azo Dye Decolorization in Aqueous Solution through Vibrating Piezoelectric Microfibers, J Phys Chem C, 116 (2012) 13045-13051.

[88] X.L. Xu, Y.M. Jia, L.B. Xiao, Z. Wu, Strong vibration-catalysis of ZnO nanorods for dye wastewater decolorization via piezo-electro-chemical coupling, Chemosphere, 193 (2018) 1143-1148.

[89] H. Lin, Z. Wu, Y. Jia, W. Li, R.-K. Zheng, H. Luo, Piezoelectrically induced mechano-catalytic effect for degradation of dye wastewater through vibrating Pb(Zr0.52Ti0.48)O3 fibers, Appl Phys Lett, 104 (2014) 162907.

[90] K. Vajda, K. Mogyorosi, Z. Nemeth, K. Hernadi, L. Forro, A. Magrez, A. Dombi, Photocatalytic activity of TiO2/SWCNT and TiO2/MWCNT nanocomposites with different carbon nanotube content, Physica Status Solidi, 248 (2011) 2496–2499.

[91] Z. Zhang, T. Zheng, X. Li, J. Xu, H. Zeng, Progress of Carbon Quantum Dots in Photocatalysis Applications, Particle & Particle Systems Characterization, 33 (2016) 457-472.

[92] W. Han, Z. Li, Y. Li, X. Fan, F. Zhang, G. Zhang, W. Peng, The Promoting Role of Different Carbon Allotropes Cocatalysts for Semiconductors in Photocatalytic Energy Generation and Pollutants Degradation, Frontiers in Chemistry, 5 (2017) 10.3389/fchem.2017.00084.

[93] S.J. Li, M. Zhang, Y.L. Gao, B.S. Bao, S.L. Wang, ZnO-Zn/CNT hybrid film as light-free nanocatalyst for degradation reaction, Nano Energy, 2 (2013) 1329-1336.

[94] Y.L. Gao, S.J. Li, B.G. Zhao, Q.J. Thai, A. Lita, N.S. Dalal, H.W. Kroto, S.F.A. Acquah, A synergistic approach to light-free catalysis using zinc oxide embedded multi-walled carbon nanotube paper, Carbon, 77 (2014) 705-709.

[95] M.D. Nguyen, E.P. Houwman, H.Y. Yuan, B.J.W.V. Eerd, M. Dekkers, G. Koster, J.E. ten Elshof, G. Rijnders, Controlling Piezoelectric Responses in Pb(Zr0.52Ti0.48)O-3 Films through Deposition Conditions and Nanosheet Buffer Layers on Glass, Acs Appl Mater Inter, 9 (2017) 35947-35957.

[96] A.C. Tas, Preparation of lead zirconate titanate (Pb(Zr0.52Ti0.48)O-3) by homogeneous precipitation and calcination, J Am Ceram Soc, 82 (1999) 1582-1584.

[97] H.Y. Zhu, Y. Wang, J. Xiao, M. Liu, S.M. Xiong, Z.J. Wong, Z.L. Ye, Y. Ye, X.B. Yin, X. Zhang, Observation of piezoelectricity in free-standing monolayer MoS2, Nat Nanotechnol, 10 (2015) 151-155.

[98] J.M. Wu, W.E. Chang, Y.T. Chang, C.K. Chang, Piezo-Catalytic Effect on the Enhancement of the Ultra-High Degradation Activity in the Dark by Single- and Few-Layers MoS2 Nanoflowers, Adv Mater, 28 (2016) 3718-3725.

[99] M.H. Wu, J.T. Lee, Y.J. Chung, M. Srinivaas, J.M. Wu, Ultrahigh efficient degradation activity of single- and few-layered MoSe2 nanoflowers in dark by piezo-catalyst effect, Nano Energy, 40 (2017) 369-375.

[100] K.A.N. Duerloo, M.T. Ong, E.J. Reed, Intrinsic Piezoelectricity in Two-Dimensional Materials, J Phys Chem Lett, 3 (2012) 2871-2876.

[101] Y.H. Chang, W. Zhang, Y. Zhu, Y. Han, J. Pu, J.K. Chang, W.T. Hsu, J.K. Huang, C.L. Hsu, M.H. Chiu, T. Takenobu, H. Li, C.I. Wu, W.H. Chang, A.T.S. Wee, L.J. Li, Monolayer MoSe2 Grown by Chemical Vapor Deposition for Fast Photodetection, Acs Nano, 8 (2014) 8582-8590.

[102] S.K. Singh, H. Ishiwara, K. Maruyama, Room temperature ferroelectric properties of Mn-substituted BiFeO3 thin films deposited on Pt electrodes using chemical solution deposition, Applied Physics Letters, 88 (2006) 262908.

[103] H. You, Y. Jia, Z. Wu, X. Xu, W. Qian, Y. Xia, M. Ismail, Strong piezo-electrochemical effect of multiferroic BiFeO3 square micro-sheets for mechanocatalysis, Electrochemistry Communications, 79 (2017) 55-58.

[104] Z.L. Wang, On Maxwell's displacement current for energy and sensors: the origin of nanogenerators, Materials Today, 20 (2017) 74-82.

[105] Y.W. Feng, L.L. Ling, Y.X. Wang, Z.M. Xu, F.L. Cao, H.X. Li, Z.F. Bian, Engineering spherical lead zirconate titanate to explore the essence of piezo-catalysis, Nano Energy, 40 (2017) 481-486.

[106] S.Y. Lan, J.X. Feng, Y. Xiong, S.H. Tian, S.W. Liu, L.J. Kong, Performance and Mechanism of Piezo-Catalytic Degradation of 4-Chlorophenol: Finding of Effective Piezo-Dechlorination, Environ Sci Technol, 51 (2017) 6560-6569.

[107] L. Simon-Seveyrat, A. Hajjaji, Y. Emiane, B. Guiffard, D. Guyomar, Re-investigation of synthesis of BaTiO3 by conventional solid-state reaction and oxalate coprecipitation route for piezoelectric applications, Ceram Int, 33 (2007) 35-40.

[108] A. Koka, H.A. Sodano, High-sensitivity accelerometer composed of ultra-long vertically aligned barium titanate nanowire arrays, Nat Commun, 4 (2013) 2682.

[109] S.C. Tu, H.W. Huang, T.R. Zhang, Y.H. Zhanga, Controllable synthesis of multi-responsive ferroelectric layered perovskite-like Bi4Ti3O12: Photocatalysis and piezoelectric-catalysis and mechanism insight, Appl Catal B-Environ, 219 (2017) 550-562.

[110] W. Lv, L.J. Kong, S.Y. Lan, J.X. Feng, Y. Xiong, S.H. Tian, Enhancement effect in the piezoelectric degradation of organic pollutants by piezo-Fenton process, J Chem Technol Biot, 92 (2017) 152-156.

[111] J.A.O. Mendez, J.A.H. Melian, J. Arana, J.M.D. Rodriguez, O.G. Diaz, J.P. Pena, Detoxification of waters contaminated with phenol, formaldehyde and phenol-formaldehyde mixtures using a combination of biological treatments and advanced oxidation techniques, Appl Catal B-Environ, 163 (2015) 63-73.

[112] J. Fernandez, J. Bandara, A. Lopez, P. Buffat, J. Kiwi, Photoassisted Fenton degradation of nonbiodegradable azo dye (Orange II) in Fe-free solutions mediated by cation transfer membranes, Langmuir, 15 (1999) 185-192.

[113] H.L. Zhou, Y.Q. Qu, T. Zeid, X.F. Duan, Towards highly efficient photocatalysts using semiconductor nanoarchitectures, Energ Environ Sci, 5 (2012) 6732-6743.

[114] J. Bandara, C.C. Hadapangoda, W.G. Jayasekera, TiO2/MgO composite photocatalyst: the role of MgO in photoinduced charge carrier separation, Appl Catal B-Environ, 50 (2004) 83-88.

[115] R. Fagan, D.E. McCormack, D.D. Dionysiou, S.C. Pillai, A review of solar and visible light active TiO2 photocatalysis for treating bacteria, cyanotoxins and contaminants of emerging concern, Mat Sci Semicon Proc, 42 (2016) 2-14.

[116] H.R. Dong, G.M. Zeng, L. Tang, C.Z. Fan, C. Zhang, X.X. He, Y. He, An overview on limitations of TiO2-based particles for photocatalytic degradation of organic pollutants and the corresponding countermeasures, Water Res, 79 (2015) 128-146.

[117] X. Han, M.X. Chen, C.F. Pan, Z.L. Wang, Progress in piezo-phototronic effect enhanced photodetectors, J Mater Chem C, 4 (2016) 11341-11354.

[118] F. Zhang, Y. Ding, Y. Zhang, X.L. Zhang, Z.L. Wang, Piezo-phototronic Effect Enhanced Visible and Ultraviolet Photodetection Using a ZnO-CdS Core-Shell Micro/nanowire, Acs Nano, 6 (2012) 9229-9236.

[119] Y.F. Hu, Y.L. Chang, P. Fei, R.L. Snyder, Z.L. Wang, Designing the Electric Transport Characteristics of

ZnO Micro/Nanowire Devices by Coupling Piezoelectric and Photoexcitation Effects, Acs Nano, 4 (2010) 1234-1240.

[120] C. Sun, Y.M. Fu, Q. Wang, L.L. Xing, B.D. Liu, X.Y. Xue, Ultrafast piezo-photocatalytic degradation of organic pollutions by Ag2O/tetrapod-ZnO nanostructures under ultrasonic/UV exposure, Rsc Adv, 6 (2016) 87446-87453.

[121] H.D. Li, Y.H. Sang, S.J. Chang, X. Huang, Y. Zhang, R.S. Yang, H.D. Jiang, H. Liu, Z.L. Wang, Enhanced Ferroelectric-Nanocrystal-Based Hybrid Photocatalysis by Ultrasonic-Wave-Generated Piezophototronic Effect, Nano Lett, 15 (2015) 2372-2379.

[122] D. Sarkar, C.K. Ghosh, S. Mukherjee, K.K. Chattopadhyay, Three Dimensional Ag2O/TiO2 Type-II (p-n) Nanoheterojunctions for Superior Photocatalytic Activity, Acs Appl Mater Inter, 5 (2013) 331-337.

[123] H.G. Yu, R. Liu, X.F. Wang, P. Wang, J.G. Yu, Enhanced visible-light photocatalytic activity of Bi2WO6 nanoparticles by Ag2O cocatalyst, Appl Catal B-Environ, 111 (2012) 326-333.

[124] G. Mamba, J. Kiwi, C. Pulgarin, R. Sanjines, S. Giannakis, S. Rtimi, Evidence for the degradation of an emerging pollutant by a mechanism involving iso-energetic charge transfer under visible light, Applied Catalysis B: Environmental, 233 (2018) 175-183.

[125] X.Y. Xue, W.L. Zang, P. Deng, Q. Wang, L.L. Xing, Y. Zhang, Z.L. Wang, Piezo-potential enhanced photocatalytic degradation of organic dye using ZnO nanowires, Nano Energy, 13 (2015) 414-422.

[126] J.H. Chang, H.N. Lin, Exploitation of piezoelectricity for enhancing photocatalytic activity of ZnO nanowires, Mater Lett, 132 (2014) 134-137.

[127] D.Y. Hong, W.L. Zang, X. Guo, Y.M. Fu, H.X. He, J. Sun, L.L. Xing, B.D. Liu, X.Y. Xue, High Piezo-photocatalytic Efficiency of CuS/ZnO Nanowires Using Both Solar and Mechanical Energy for Degrading Organic Dye, Acs Appl Mater Inter, 8 (2016) 21302-21314.

[128] Y. Zhang, C.H. Liu, G.L. Zhu, X. Huang, W. Liu, W.G. Hu, M. Song, W.D. He, J. Liu, J.Y. Zhai, Piezotronic-effect-enhanced Ag2S/ZnO photocatalyst for organic dye degradation, Rsc Adv, 7 (2017) 48176-48183.

[129] L.L. Zhang, D. Zhu, H.X. He, Q. Wang, L.L. Xing, X.Y. Xue, Enhanced piezo/solar-photocatalytic activity of Ag/ZnO nanotetrapods arising from the coupling of surface plasmon resonance and piezophototronic effect, J Phys Chem Solids, 102 (2017) 27-33.

[130] G.R.S. Andrade, C.C. Nascimento, E.C. Silva, D.T.S.L. Mendes, I.F. Gimenez, ZnO/Au nanocatalysts for enhanced decolorization of an azo dye under solar, UV-A and dark conditions, J Alloy Compd, 710 (2017) 557-566.

[131] Y.M. Dong, C.Y. Feng, P.P. Jiang, G.L. Wang, K. Li, H.Y. Miao, Simple one-pot synthesis of ZnO/Ag heterostructures and the application in visible-light-responsive photocatalysis, Rsc Adv, 4 (2014) 7340-7346.

[132] H.L. You, Z. Wu, Y.M. Jia, X.L. Xu, Y.T. Xia, Z.C. Han, Y. Wang, High-efficiency and mechano-/photo-bi-catalysis of piezoelectric-ZnO@ photoelectric-TiO2 core-shell nanofibers for dye decomposition, Chemosphere, 183 (2017) 528-535.

[133] L.F. Wang, S.H. Liu, Z. Wang, Y.L. Zhou, Y. Qin, Z.L. Wang, Piezotronic Effect Enhanced Photocatalysis in Strained Anisotropic ZnO/TiO2 Nanoplatelets via Thermal Stress, Acs Nano, 10 (2016) 2636-2643.

[134] E.A. Serna-Galvis, J. Silva-Agredo, A.L. Giraldo-Aguirre, O.A. Flórez-Acosta, R.A. Torres-Palma, High frequency ultrasound as a selective advanced oxidation process to remove penicillinic antibiotics and eliminate its antimicrobial activity from water, Ultrasonics sonochemistry, 31 (2016) 276-283.

[135] E.A. Serna-Galvis, J. Silva-Agredo, A.L. Giraldo, O.A. Flórez, R.A. Torres-Palma, Comparison of route, mechanism and extent of treatment for the degradation of a β-lactam antibiotic by TiO2 photocatalysis, sonochemistry, electrochemistry and the photo-Fenton system, Chemical Engineering Journal, 284 (2016)

953-962.

[136] B.Y. Dai, H.M. Huang, W. Wang, Y.K. Chen, C.H. Lu, J.H. Kou, L.Z. Wang, F.L. Wang, Z.Z. Xu, Greatly enhanced photocatalytic activity by organic flexible piezoelectric PVDF induced spatial electric field, Catal Sci Technol, 7 (2017) 5594-5601.

[137] Z.M. Dang, Y.H. Lin, C.W. Nan, Novel ferroelectric polymer composites with high dielectric constants, Adv Mater, 15 (2003) 1625-+.

[138] A. Jain, K.J. Prashanth, A.K. Sharma, A. Jain, P.N. Rashmi, Dielectric and piezoelectric properties of PVDF/PZT composites: A review, Polym Eng Sci, 55 (2015) 1589-1616.

[139] C.Y. Dong, Y.M. Fu, W.L. Zang, H.X. He, L.L. Xing, X.Y. Xue, Self-powering/self-cleaning electronic-skin basing on PVDF/TiO2 nanofibers for actively detecting body motion and degrading organic pollutants, Appl Surf Sci, 416 (2017) 424-431.

[140] H.X. He, Y.M. Fu, W.L. Zang, Q. Wang, L.L. Xing, Y. Zhang, X.Y. Xue, A flexible self-powered T-ZnO/PVDF/fabric electronic-skin with multi functions of tactile-perception, atmosphere-detection and self-clean, Nano Energy, 31 (2017) 37-48.

[141] H.W. Huang, S.C. Tu, C. Zeng, T.R. Zhang, A.H. Reshak, Y.H. Zhang, Macroscopic Polarization Enhancement Promoting Photo- and Piezoelectric-Induced Charge Separation and Molecular Oxygen Activation, Angew Chem Int Edit, 56 (2017) 11860-11864.

[142] H.W. Huang, X.W. Li, X. Han, N. Tian, Y.H. Zhang, T.R. Zhang, Moderate band-gap-broadening induced high separation of electron-hole pairs in Br substituted BiOI: a combined experimental and theoretical investigation, Phys Chem Chem Phys, 17 (2015) 3673-3679.

[143] H.W. Huang, R.R. Cao, S.X. Yu, K. Xu, W.C. Hao, Y.G. Wang, F. Dong, T.R. Zhang, Y.H. Zhang, Single-unit-cell layer established Bi2WO6 3D hierarchical architectures: Efficient adsorption, photocatalysis and dye-sensitized photoelectrochemical performance, Appl Catal B-Environ, 219 (2017) 526-537.

[144] P. Madhusudan, J.G. Yu, W.G. Wang, B. Cheng, G. Liu, Facile synthesis of novel hierarchical graphene-Bi2O2CO3 composites with enhanced photocatalytic performance under visible light, Dalton T, 41 (2012) 14345-14353.

[145] H.W. Huang, S.C. Tu, X. Du, Y.H. Zhang, Ferroelectric spontaneous polarization steering charge carriers migration for promoting photocatalysis and molecular oxygen activation, J Colloid Interf Sci, 509 (2018) 113-122.

[146] L. Hao, H.W. Huang, Y.X. Guo, Y.H. Zhang, Multifunctional Bi2O2(OH)(NO3) Nanosheets with {001} Active Exposing Facets: Efficient Photocatalysis, Dye-Sensitization, and Piezoelectric-Catalysis, Acs Sustain Chem Eng, 6 (2018) 1848-1862.

[147] B.Y. Dai, C.H. Lu, J.H. Kou, Z.Z. Xu, F.L. Wang, Photocatalytic performance of PMN-PT@TiO2 highly enhanced by alternative spatial electric field induced charge separation effect, Journal of Alloys and Compounds, 696 (2017) 988-995.

[148] P. Kumar, S. Singh, O.P. Thakur, C. Prakash, T.C. Goel, Study of lead magnesium niobate-lead titanate ceramics for piezo-actuator applications, Jpn J Appl Phys 1, 43 (2004) 1501-1506.

[149] S.Y. Xu, Y.W. Yeh, G. Poirier, M.C. McAlpine, R.A. Register, N. Yao, Flexible Piezoelectric PMN-PT Nanowire-Based Nanocomposite and Device, Nano Lett, 13 (2013) 2393-2398.

[150] B.Y. Dai, L. Zhang, H.M. Huang, C.H. Lu, J.H. Kou, Z.Z. Xu, Photocatalysis of composite film PDMS-PMN-PT@TiO2 greatly improved via spatial electric field, Appl Surf Sci, 403 (2017) 9-14.

[151] J.M. Wu, C. Xu, Y. Zhang, Y. Yang, Y.S. Zhou, Z.L. Wang, Flexible and Transparent Nanogenerators Based on a Composite of Lead-Free ZnSnO3 Triangular-Belts, Adv Mater, 24 (2012) 6094-+.

[152] H. Gou, J. Zhang, Z. Li, G. Wang, F. Gao, R.C. Ewing, J. Lian, Energetic stability, structural transition, and

thermodynamic properties of ZnSnO3, Appl Phys Lett, 98 (2011) 091914.

[153] M.K. Lo, S.Y. Lee, K.S. Chang, Study of ZnSnO3-Nanowire Piezophotocatalyst Using Two-Step Hydrothermal Synthesis, J Phys Chem C, 119 (2015) 5218-5224.

[154] Y.T. Wang, K.S. Chang, Piezopotential-Induced Schottky Behavior of Zn1-xSnO3 Nanowire Arrays and Piezophotocatalytic Applications, J Am Ceram Soc, 99 (2016) 2593-2600.

[155] H.M. Lin, K.S. Chang, Synergistic piezophotocatalytic and photoelectrochemical performance of poly(vinylidene fluoride)-ZnSnO3 and poly(methyl methacrylate)-ZnSnO3 nanocomposites, Rsc Adv, 7 (2017) 30513-30520.

[156] S. Singh, N. Khare, Coupling of piezoelectric, semiconducting and photoexcitation properties in NaNbO3 nanostructures for controlling electrical transport: Realizing an efficient piezo-photoanode and piezo-photocatalyst, Nano Energy, 38 (2017) 335-341.

[157] N. Ahner, D. Gottschlich, S. Narang, D. Roberts, S. Sharma, S. Ventura, Piezoelectrically Assisted Ultrafiltration, Separ Sci Technol, 28 (1993) 895-908.

[158] H.G.L. Coster, T.D. Farahani, T.C. Chilcott, Production and characterization of piezo-electric membranes, Desalination, 283 (2011) 52-57.

[159] M.T. Darestani, H.G.L. Coster, T.C. Chilcott, Piezoelectric membranes for separation processes: Operating conditions and filtration performance, J Membrane Sci, 435 (2013) 226-232.

[160] M.T. Darestani, H.G.L. Coster, T.C. Chilcott, S. Fleming, V. Nagarajan, H. An, Piezoelectric membranes for separation processes: Fabrication and piezoelectric properties, J Membrane Sci, 434 (2013) 184-192.

[161] J.K. Krinks, M.H. Qiu, I.A. Mergos, L.K. Weavers, P.J. Mouser, H. Verweij, Piezoceramic membrane with built-in ultrasonic defouling, J Membrane Sci, 494 (2015) 130-135.

[162] J. Bae, I. Baek, H. Choi, Efficacy of piezoelectric electrospun nanofiber membrane for water treatment, Chem Eng J, 307 (2017) 670-678.

[163] D. Kuscer, T. Rojac, D. Belavic, M.S. Zarnik, A. Bradesko, T. Kos, B. Malic, M. Boerrigter, D.M. Martin, M. Faccini, Integrated piezoelectric vibration system for fouling mitigation in ceramic filtration membranes, J Membrane Sci, 540 (2017) 277-284.

[164] M.B. Starr, J. Shi, X.D. Wang, Piezopotential-Driven Redox Reactions at the Surface of Piezoelectric Materials, Angew Chem Int Edit, 51 (2012) 5962-5966.

[165] J. Zhang, Z. Wu, Y.M. Jia, J.W. Kan, G.M. Cheng, Piezoelectric Bimorph Cantilever for Vibration-Producing-Hydrogen, Sensors-Basel, 13 (2013) 367-374.